Novel Approaches to Studying *BRCA* Variants of Unknown Clinical Significance

by
Rory L. Cochran

A dissertation submitted to Johns Hopkins University in conformity with the requirements for the degree of Doctor of Philosophy

Baltimore, Maryland
August 2014

Abstract

Hereditary breast cancer comprises ~7% of the annual breast cancer cases in the United States. The two genes suspected in the majority of cases are the breast and ovarian cancer susceptibility genes 1 and 2 (*BRCA1* and *BRCA2*). Although *BRCA* genetic testing has aided in the identification of specific individuals at risk for breast and ovarian cancer, the large number of *BRCA* variants of unknown clinical significance (VUS) continues to complicate prevention strategies. To augment the ongoing VUS classification effort, two novel approaches for studying *BRCA* VUS were developed. First, an isogenic panel of immortalized human breast cells harboring eight different clinically reported *BRCA1* alleles were established to study genomic instability. Consistent with previous findings, cells harboring a deleterious allele (185delAG, C61G and R71G) demonstrate increased ɣ-irradiation sensitivity and genomic instability, as measured by fluorescent *in situ* hybridization. Interestingly, not all deleterious alleles demonstrated the same level of haploinsufficiency, as each genotype exhibited varying degrees of change from the control cell lines across different assays. Second, an improved approach for studying *BRCA* variant loss-of-heterozygosity (LOH) within archival tumor tissue was developed. Using a new digital PCR platform, droplet digital PCR (ddPCR), *BRCA2* LOH was assessed in formalin fixed paraffin embedded (FFPE) tissues for two related breast cancer patients harboring a rare missense *BRCA2* variant of unknown clinical significance (c.6966G>T; M2322I). Conventional PCR followed by Sanger sequencing suggested a change in allelic abundance in the FFPE specimens. However, there was no evidence of LOH as determined by the allelic ratio (wild type:variant) for *BRCA2* in both patients' archival tumor specimens and adjacent normal control tissues using ddPCR. In summary,

these experiments demonstrate two novel approaches for studying the clinical significance of uncertain *BRCA* alleles.

Thesis Advisor: Ben Ho Park, MD., Ph.D.

Thesis Readers: Ben Ho Park, MD., Ph.D.
Josh Lauring, MD., Ph.D.

Acknowledgements

At this stage in my academic training there are countless individuals towards whom I feel obliged to express my deepest gratitude. For without their mentorship, help, advice, love and overall support, this dissertation would almost certainly not exist. Indeed, a separate work altogether could be written aimed solely at thanking the numerous people that have fostered my education and enabled this work to materialize. So, in the interest of brevity, I would like to convey an encompassing thank you to all my colleagues, friends and family.

There are, of course, certain people that have made significant impacts on my growth as a person and as a scientist, for whom I feel it requisite to specifically thank here. Firstly, I would like to thank my phenomenal parents, Ronald and Theresa Cochran, for their unlimited love and support. Your personal qualities are to be admired and your love for one another is to be emulated. Mom, your innate inclination to treat others with unconditional kindness and respect has inspired me to spend a life caring for others and researching cures for disease. And Dad, your personal integrity and example of what it means to have a fierce work ethic has taught me not only self-reliance, but also that all things worthwhile in life come through honest hard work and perseverance. I am the person I am today because of the both of you, and I am extremely grateful, *thank you*.

Like all graduate students, many different individuals have fostered my growth as a scientist, so I would like to express my sincerest thanks to those people as well. A special thanks goes out to Drs. Palmer Taylor, Zoran Radić and Jeremy Babendure for giving me the opportunity to try my hand at laboratory science. I would also like to thank

my colleagues and friends at the Johns Hopkins University School of Medicine. More specifically, I would like to thank the Cellular & Molecular Medicine graduate program administrators, Colleen Graham and Leslie Lichter, and director, Dr. Rajini Rao, for their unparalleled support. Thank you for providing me the outstanding opportunity to come to Hopkins for my graduate training.

Passionately, I would also like to thank all the current and past members of the Ben Ho Park and Josh Lauring labs. You have made my tenure at Hopkins one I will never forget. A special thank you goes out to Dr. Josh Lauring for his helpful suggestions and thoughtful discussions over the many weekends in lab. And, of course, an earnest thank you goes out to my thesis advisor, Dr. Ben Ho Park, for his boundless support. Ben, you are an exemplar role model, physician, scientist, mentor and friend. Thank you for always being marvelously patient with my impatience. If I am fortunate enough to have a lab of my own in the future, I feel I will be well equipped if I am half the mentor and scientist you are. I am honored to call you my friend and will always consider you a member of my family.

Lastly, and absolutely not least, I would like to thank my spouse, Kristi Cochran, for her unwavering love, patience and support. Moving three thousand miles away from our home in San Diego was certainly not easy, but having you by my side has made these past years worthwhile. Kristi, you give me strength in times of need and remind me to stop and enjoy life. I am excited about the next chapter of our lives and I am honored you have chosen me to be your spouse. *I love you*.

Table of Contents

List of Tables

List of Figures

Figure 3.6: Representative ddPCR results

1 Introduction

Discovery of *BRCA1* & *BRCA2*

Breast cancer is caused by the accumulation of somatic mutations in the DNA of mammary epithelial cells (1). Although the majority of cancers are sporadic, caused by spontaneous DNA mutations, a subset of annual cases are linked to the transmission of susceptibility factors (2). Yet, decades before the discovery of the genes responsible for causing familial breast cancer, clinicians made several observations that aided in their discovery. Physicians noted that for some individuals, breast cancer onset was remarkably early in life and often these individuals had a higher incidence of multiple primary tumors. Additionally, these patients routinely had extensive family histories of cancer, sometimes including male breast cancers (3). Utilizing these important features to identify suspect families, investigators eventually identified the principal genes responsible for influencing hereditary breast cancer onset (4). It is now commonly accepted that the two major genes responsible for predisposing individuals to breast and

ovarian cancer are *BRCA1* and *BRCA2,* both of which were cloned in the mid-1990s. Other lower frequency genes known to influence familial breast cancer susceptibility, including *PTEN*, *CDH1*, *ATM, CHEK2, PALB2* and *STK11* are reviewed elsewhere (2).

In 1990, *BRCA1* was first mapped to human chromosome 17q using linkage analysis in a series of 23 large kindreds with the archetypal breast cancer family history (5). At the time, it was hypothesized that *BRCA1* was an autosomal dominant tumor suppressor gene, and therefore, should follow the classical two hit hypothesis previously described by Alfred Knudson (6). Consistent with the theory, somatic allelic losses were predicted to occur at 17q at some frequency in both hereditary and sporadic tumors. Indeed, shortly after the localization of *BRCA1* to 17q, researchers published reports demonstrating genomic losses on 17q in both sporadic and familial breast cancer (7, 8). It was not until several years later, after laborious effort, was the *BRCA1* gene finally isolated using positional cloning (9). Again, consistent with the contemporary notion that *BRCA1* was a tumor suppressor gene and should follow the two hit hypothesis (6), somatic loss of the remaining wild-type allele was observed in the tumors of patients harboring germ line *BRCA1* mutations. Paradoxically, however, somatic mutations resulting in complete loss of function of *BRCA1* were rarely observed in sporadic breast cancers (10). This led researchers to speculate that other mechanisms for reducing BRCA1 expression may be involved, such as epigenetic gene silencing through methylation of the *BRCA1* promoter (11).

Notably, germ line *BRCA1* mutations were not observed in purported cancer families with male breast cancer (12) and *BRCA1* did not seem to account for all families displaying an autosomal dominant pattern of breast and ovarian cancer inheritance. These

observations led investigators to search for other causative genes culminating in the localization of *BRCA2* to human chromosome 13q in 1994 (13) and ultimately its identification a year later (14). Similar to the genetics of *BRCA1,* and again consistent with being a tumor suppressor gene, somatic loss of the remaining wild-type *BRCA2* allele was observed in a significant number of patient tumors with a germ line *BRCA2* mutation (15). In contrast to *BRCA1*, however, transmission of a deleterious *BRCA2* allele also appears to increase the risk of developing cancers outside the breast and ovaries, particularly cancers of the pancreas and prostate (16, 17). Additionally, certain germ line homozygous mutations in *BRCA2* cause the rare autosomal recessive disease, Fanconi anemia (18).

Soon after the discovery of the *BRCA* genes it became apparent that both were highly polymorphic. Therefore, to manage the growing number of discovered germ line *BRCA* alleles and bolster research efforts, the Breast Cancer Information Core (BIC) was established in 1995 (19). As of the writing of this thesis, the BIC catalogs >1,800 unique *BRCA1* alleles and >2,000 *BRCA2* alleles. Within the BIC three types of clinical designations exist for the cataloged alleles: deleterious, benign and unknown variant. Deleterious alleles comprise ~50% and ~41% of the cataloged *BRCA1* and *BRCA2* alleles, respectively. Most of the deleterious alleles are the result of frame-shift or truncating mutations, having obvious adverse effects on the translated protein products. Unfortunately, ~48% and ~56% of the cataloged *BRCA1* and *BRCA2* alleles, respectively, are considered variants of unknown clinical significance (VUS). Most VUS are comprised of missense, intronic and regulatory region mutations with unclear phenotypic consequences. The existence of the large number of VUS has catalyzed many research

efforts aimed at determining their clinical significance and are discussed in more detail below.

Gene Structure & Protein Domains

In addition to being highly polymorphic, both *BRCA1* and *BRCA2* are very large genes, encoding very large proteins. Several BRCA1 isoforms have been reported to exist within cells. The most commonly studied isoform spans 23 exons and encodes a protein 1,863 amino acids in size (~220 kD), located predominately within the nucleus (9, 20). A splice variant arising from the same transcript, but lacking the majority of exon 11 has also been reported (~110 kD) (21). This isoform, termed BRCA1-Δ11b, accumulates in the cytoplasm because it lacks its exon 11 encoded nuclear localization signals. A decade ago, another group published a report claiming the existence of a unique functionally important isoform, termed BRCA1-IRIS, resulting from an uninterrupted reading frame starting from exon 1 extending into intron 11 (22). In spite of multiple BRCA1 isoform reports, the majority of studies to date focus on the 220 kD BRCA1 (p220) protein. Therefore, any mention here of the BRCA1 protein refers to the p220 isoform, unless otherwise stated.

Two important, evolutionarily conserved functional domains exist within BRCA1: the N-terminal RING motif and the C-terminal tandem BRCT motifs. Both domains appear to be essential for BRCA1 mediated tumor suppression, as known cancer causing mutations have been identified in each (9, 23–25). Interestingly, the BRCA1 C-Terminal (BRCT) domain was originally identified through a bioinformatics approach (26). Using protein BLAST, Koonin et al. reported that two other nuclear proteins,

53BP1 and RAD9, share what appeared to be a conserved protein domain, which they named after BRCA1. Using an alternative sequence analysis approach, hydrophobic cluster analysis, another group subsequently identified several other nuclear proteins possessing BRCT domains (27). Present data support the notion that at least for certain BRCT superfamily members, including BRCA1, the BRCT domain acts as a phosphopeptide binding module important for mediating the DNA damage response (28, 29). Currently, over two-dozen proteins harboring a BRCT domain have been identified with most having some role in either cell cycle checkpoint control and/or the DNA damage repair response (30, 31).

The other well studied BRCA1 motif, the N-terminal zinc finger RING domain, was also originally identified by querying a contemporary sequence database (9, 32). RING domains are one of two major types of domains found in the superfamily of E3 ubiquitin ligases. Perhaps not surprisingly, BRCA1's RING domain is important for mediating its confirmed E3 ubiquitin ligase activity (33–35). In addition, BRCA1's RING domain mediates heterodimer formation with its binding partner, BARD1 (36). The importance of BRCA1/BARD1 heterodimer formation is underscored by the presence of known cancer causing mutations located within the RING domain, disrupting normal tertiary structure necessary for interaction between the two proteins (37). Heterodimer formation enhances BRCA1's E3 ligase activity (33, 34) and appears to be mutually important for each protein's stability within cells (38). Although the RING domain appears to be required for tumor suppression (39), it remains controversial whether BRCA1's ubiquitin ligase activity is required for tumor suppression in humans, as conflicting data currently exists (40–42).

Distinct from *BRCA1*, the *BRCA2* gene located on the long arm of human chromosome 13 spans 27 exons encoding a protein 3,418 amino acids in size (380 kD) (43). Their appears to be only one BRCA2 isoform and it is found predominately within the nucleus (44). Currently, only two corroborated functional domains have been described for BRCA2: the evolutionarily conserved eight BRC repeat motifs encoded within exon 11 and the C-terminal domain that harbors its nuclear localization signals. Similar to cancer mutations found in the two conserved functional domains of BRCA1, known cancer causing mutations are found in the two important functional domains of BRCA2, again underscoring their importance for normal BRCA2 tumor suppressor function (45, 46).

Function

BRCA1 appears to be a pleiotropic mammalian gene with multiple functions now ascribed to its gene products. BRCA1 has been implicated in transcriptional regulation (47, 48), DNA repair (49, 50), cell-cycle checkpoint control (51, 52), centrosome dynamics (53–56) and epigenetic regulation (41, 57). In fact, the complete cellular function of *BRCA1* remains an area of continued research. Therefore, for clarity, only BRCA1's established role in maintaining genome integrity will be discussed further. More specifically, BRCA1's critical role in maintaining genomic stability through both regulation of centrosome duplication and its multi-faceted role in the DNA damage response and repair pathway will be discussed.

The earliest indication that BRCA1 may play a critical role in cells came through knock-out mice studies evaluating different *BRCA1* genotypes. Initially, researchers

observed that homozygous germ-line disruption of *BRCA1* was incompatible with normal murine development and led to embryonic lethality (58–60). Interestingly, the different *BRCA1* functional domains that were disrupted in each of these transgenic studies led to temporal differences in developmental termination, suggesting BRCA1 may harbor distinct functional domains critical at different stages of normal murine development. At the time, these findings seemed somewhat paradoxical since many believed that BRCA1 loss of function would be permissive as it is frequently observed in *BRCA1*-associated tumorigenesis. It is important to note, however, that none of the monogenic knock-out mice studies to date have observed any increase in mammary tumor incidence for $BRCA1^{+/-}$ heterozygous mice. This may be due to the inherently shorter lifespan of mice and/or the limited follow up time within these studies. An alternative explanation is that important species-specific differences exist between humans and mice. Consistent with this theory, there appear to be no observable phenotypes associated in murine $BRCA1^{+/-}$ heterozygous mammary cells, contrasting to the reports claiming that *BRCA1* haploinsufficiency may exist in certain human tissues (61–64). Is biallelic inactivation of *BRCA1* embryonic lethal for humans as well? As of this writing, there appear to be only two publications to date reporting the presence of individuals with germ line homozygous *BRCA1* deleterious mutations (65, 66). The first article reporting a women with a homozygous *BRCA1* founder mutation (c.2800delAA) has since been refuted, as it seems the author's genotypic conclusions were based on the result of a PCR artifact (65, 67, 68). The second article, published recently, describes a cancer affected women harboring one deleterious allele (c.2457delC) and one VUS allele (V1736A) (66). The proband was diagnosed at age 28 years with stage IV papillary serous ovarian carcinoma, and she had

a clinical history of both microcephaly and short stature. In their report, the authors provide strong evidence that the VUS may be a hypomorphic allele. Therefore, until proven otherwise, it seems that complete loss of BRCA1 function is incompatible with normal human embryogenesis as well.

BRCA1's role in the repair of DNA double strand breaks has been extensively studied (49). Early evidence for this function arose from studies of BRCA1's unique nuclear staining pattern, and BRCA1 was found to co-immunoprecipitate with the DNA recombination factor, RAD51 (69). BRCA1's suspected role in DNA repair was quickly confirmed by the observation that mouse embryonic stem cells lacking BRCA1 were deficient in DNA repair by homologous recombination (49). Bolstering this finding, another group found that exogenous expression of wild-type BRCA1 suppressed radiation hypersensitivity using a newly established human cancer cell line derived from a *BRCA1* deleterious mutation carrier (70, 71). The cancer cell line (HCC1937) utilized in this study lacked normal BRCA1 function resulting from the presence of a germ line *BRCA1* mutation (5382insC) with loss of the remaining wild-type allele. Since these groundbreaking discoveries, a vast amount of work has been carried out corroborating BRCA1's role in the repair of DNA damage. Subsequent reports suggest that BRCA1 is found in several DNA repair protein complexes involved in the homology mediated repair of different types of DNA lesions, including collapsed replication forks and cross-linked DNA (50, 72, 73).

The other established genome-maintaining function of BRCA1 is its regulatory role in centrosome dynamics. Insight into this function was also initially gleaned from studies of isolated *BRCA1* null fibroblasts from embryos of *BRCA1* homozygous knock-

out mice (53). In the study by Xu et al., significant genetic instability in the BRCA1 deficient cells was observed, which appeared to be linked, at least in part, to centrosome duplication and a defective G_2-M cell cycle checkpoint. At the time, hypothesizing that BRCA1 may somehow regulate centrosome dynamics seemed plausible, as previous immunofluorescence work suggested that BRCA1 localized to the centrosome and interacted with ɣ-tubulin (54). Similar to BRCA1 research focusing on DNA damage repair, over a decade has passed since these initial reports linking BRCA1 to centrosome dynamics with a more complete picture now existing. Briefly, the current model for BRCA1 mediated centrosome regulation stipulates that in a cell-cycle dependent manner, the BRCA1/BARD1 heterodimer ubiquitinates ɣ-tubulin preventing secondary centrosome duplication (55, 56, 74). Upon BRCA1 loss of function, cells are found to have supernumerary centrosomes, which promote genomic instability.

BRCA2's function within cells seems to be primarily restricted to the repair of DNA double strand breaks (44). Not surprisingly, the earliest evidence for BRCA2's role in DNA repair also arose through knock-out mice studies. Like *BRCA1* deficient mice, nullizygosity for *BRCA2* leads to murine embryonic lethality (75). Sharan et al., demonstrated that *BRCA2* null cells both show a marked sensitivity to ɣ-irradiation and that BRCA2 interacts with RAD51 via its BRC repeat domain. Yet BRCA2's direct role in DNA repair by homologous recombination was not confirmed until several years later by Moynahan et al. (76). In summary, a great number of reports have been published corroborating BRCA2's role in mediating the repair of DNA double strand breaks via homologous recombination, and are thoroughly reviewed elsewhere (73, 77, 78).

Clinical Features

BRCA-linked breast cancers, in contrast to sporadic breast cancers, exhibit distinct pathological characteristics. Collectively, *BRCA1*-linked disease tends to be higher grade at diagnosis with an increased number of observable mitoses compared to both *BRCA2*-linked and sporadic disease (79, 80). Approximately 70% of the *BRCA1* associated tumors do not express any of the three commonly scored breast cancer receptors (estrogen receptor [ER], progesterone receptor [PR] and human epidermal growth factor receptor 2[HER2]), designating them as 'triple negative' (81). Moreover, *BRCA1* tumors often express several cytokeratins classifying them as of the 'basal-like' gene expression subtype as well (82). In contrast to *BRCA1*, a majority of *BRCA2* tumors are often ER positive and less aggressive (81). Interestingly, the distribution and frequency of *TP53* mutations seems to be distinct within *BRCA* tumors. Indeed, not only do *TP53* mutations seem to be more common within *BRCA* related tumors, as compared to sporadic cases, truncating mutations within *TP53* seem to be favored over missense mutations (83–86).

Penetrance for *BRCA*-linked disease appears to vary widely (87–89). This is likely due to environmental effects, the influence of modifier genes and the highly polymorphic nature of the *BRCA* genes. Now, twenty years following the discovery of *BRCA1/2* and despite the large number of published reports, disease penetrance estimates remain a matter of debate (90). However, it is commonly accepted that for *BRCA1* carriers, the lifetime risk of breast cancer is approximately 60-70% and 20-40% for ovarian cancer. In addition, it is commonly accepted that *BRCA2* linked disease has reduced penetrance relative to *BRCA1* with estimates ranging from 40-60% for breast cancer and 10-20% for

ovarian cancer (91). The accepted median age at diagnosis for deleterious carriers is 40 and 43 years for *BRCA1* and *BRCA2*, respectively (81).

Not surprisingly, *BRCA* genetic testing has become an important prerequisite for disease prevention (92). To identify carriers of deleterious *BRCA* alleles, individuals demonstrating risk criteria (i.e. personal and/or family history) are regularly encouraged by their clinicians to pursue clinical genetic counseling and testing. There are four possible outcomes for patients receiving *BRCA* genotyping: i) no mutation is found, ii) a benign variant is found, iii) a deleterious mutation is found, or iv) a variant of unknown significance (VUS) is found. Obviously, outcomes i and ii suggest the individual has no increased risk of *BRCA*-linked disease. For outcome iii, individuals may then decide to pursue intensive screening or preventative treatments. Broadly, the three preventative measures include increased screening, prophylactic surgery, and chemoprevention, with surgery being the most effective. In at-risk carriers, prophylactic bilateral oophorectomy reduces the risk of breast cancer by ~50% (93) and prophylactic bilateral mastectomy reduces the risk of breast cancer by ~90% for women with their ovaries intact (94). Women who elect for both a prophylactic oophorectomy and mastectomy have a ~95% risk reduction (94). Lastly, for individuals with outcome iv, the effectiveness of preventative action is unclear.

Recent work exploring synthetic lethal interactions within *BRCA* null cells has resulted in the discovery of a new, highly targeted therapeutic approach for a broad array of cancer types, including *BRCA* tumors. In 2005, two groups simultaneously published landmark work demonstrating remarkable killing of *BRCA* null cells using both poly-ADP-ribose polymerase inhibitors (PARPi) and PARP RNA interference technology (95,

96). It appears tumor cells with deficient homology directed DNA repair require the activity of PARPs (97). These findings have catalyzed a torrent of pre-clinical and clinical studies aimed at evaluating PARPi for an array of cancers (98–102). Indeed, numerous Phase I-III clinical trials aimed at assessing several different PARPi (namely, Rucaparib, Veliparib, Olaparib, Niraparib and Iniparib) within different cancer patient populations are either completed or underway (97). Relevantly, it seems PARPi therapy may be particularly effective for certain *BRCA* mutant cancers.

Functional Approaches to Studying BRCA1 VUS

A vast number of approaches now exist for studying the effects different DNA mutations have on the BRCA proteins. These methods may be partitioned into three main categories: multi-factorial clinically-based probabilistic modeling, *in silico* analysis and directed functional testing of the isolated BRCA protein or *in vitro* testing within a defined cellular context (103–105). The current clinical methods utilize a number of clinically important factors to calculate a probability that a particular VUS is deleterious, including: allele segregation, co-occurrence of a VUS with a deleterious allele in *trans*, pathological characteristics of tumors harboring a VUS (ER/PR/HER2 status and cytokeratin expression), loss-of-heterozygosity (LOH) and the presence of multiple primary tumors within the same individual. Arguably, the clinically based approaches are the most relevant in determining variant clinical significance. However, several problems impede their application. Particularly, a large number of VUS are extremely rare, families harboring said alleles are often small, and *BRCA*-linked disease is incompletely penetrant. Coupled with the high incidence of sporadic breast cancer in the general population, these complicating factors often lead to unreliable statistical predictions. As a result,

investigators have turned to directed functional approaches to augment VUS classification efforts. The *in vitro* functional approaches will be primarily discussed here, as they are not only relevant to this dissertation but they possess the advantage of interrogating full length protein within a defined cellular context.

Most of the *in vitro* studies have primarily focused on complementation of exogenously expressed VUS in either a cell line lacking functional BRCA or by transient knockdown of BRCA using RNA interference (104, 106). The earliest report of this approach was developed for *BRCA1* by Scully et al., where it was demonstrated that exogenous expression of wild-type BRCA1 in the BRCA1 null cancer cell line HCC1937 restored resistance to ɣ-irradiation (70). Using restoration of radio-resistance as a measure of BRCA1 function, the authors went onto to test other BRCA1 mutant/variant proteins, where the authors demonstrated that only functionally competent BRCA1 was able to restore radio-resistance. This same approach was later used by Ruffner et al. to study *BRCA1* RING variants (33).

Jeffrey Parvin's group's has demonstrated that RNAi mediated knockdown of BRCA1 combined with complementation of exogenous *BRCA1* cDNA can also be useful for studying VUS function. Using a HeLa cell line derivative harboring an integrated GFP reporter that measures homologous recombination (HR), Ransburgh et al. showed that RNAi knockdown of endogenous wild-type BRCA1 with exogenous expression of various *BRCA1* cDNA can accurately test for VUS DNA repair function (107). Using this same approach in Hs578T cells, Parvin's group went onto study the effects different *BRCA1* VUS have on regulating centrosome duplication (108).

Lastly, Shyam Sharan's group at the NIH has employed an embryonic stem cell rescue approach to study *BRCA* VUS (109, 110). As mentioned above, *BRCA* nullizygosity is incompatible with normal development in mice. Using this observation, Sharan's group developed an elegant approach to assess the ability of different *BRCA* alleles to rescue mouse embryonic stem (ES) cells from death. To accomplish this, first heterozygous ES cells with only one functional copy of *BRCA* were engineered. Importantly, the intact copy of *BRCA* was manipulated to have both a flanking *HPRT1* minigene and *loxP* sites, so that upon Cre mediated removal of the intact *BRCA* gene, the resultant clones would be both HAT resistant and devoid of BRCA function. Using these ES cell derivatives (engineered for either *BRCA1* or *BRCA2*) they then introduced bacterial artificial chromosomes (BACs) harboring different *BRCA* VUS to assess each variant's ability to rescue the clones from death.

This approach has subsequently been adopted by Bouwman et al. to more efficiently study *BRCA1* VUS in a more high-throughput manner via rescue using human *BRCA1* cDNAs, instead of BACs harboring the respective human *BRCA1* VUS (111). Similar to Sharan's group, Bouwman et al. created hemizygous *BRCA1* mouse embryonic stem cells harboring a conditional *BRCA1* allele. In addition, the investigators also utilized both alleles of the *Rosa26* locus. One allele of the *Rosa26* locus was engineered to harbor a 4-hydroxytamoxifen (4-OHT) inducible Cre, permitting Cre-mediated removal of the *loxP* flanked *BRCA1* allele. And, to better control for effects due to random integration of the exogenous complementing *BRCA1* cDNA, the investigators engineered the other *Rosa26* allele to harbor F3 and *Frt* recombination sites to facilitate recombinase-mediated cassette exchange (111). With these improvements, the

investigators were able to efficiently and effectively study 74 clinically reported *BRCA1* VUS.

2 Isogenic cell modeling of *BRCA1* alleles

Introduction

As mentioned in chapter one, previous mouse studies have suggested that *BRCA1*-linked tumorigenesis may not follow the classical two-hit hypothesis outlined for tumor suppressor genes. Prerequisite mutations may be necessary for mammalian cells to tolerate bi-allelic loss of *BRCA1*. Therefore, to study the *BRCA1* heterozygous carrier state, our lab previously performed somatic cell gene targeting in two non-tumorigenic breast epithelial cell lines: MCF-10A and an hTERT immortalized mammary epithelial cell line acquired from the Myles Brown lab (112, 113). In this study we chose to engineer cells with the most common deleterious *BRCA1* mutation, the Ashkenazi founder mutation, $BRCA1^{185delAG}$ (62). Using several different approaches, we found that the engineered cells manifested several characteristics reminiscent of the distinct features commonly observed in *BRCA1* null cancer cells, albeit to a lesser degree. In particular,

our *BRCA1* heterozygous cells demonstrated slowed proliferation, an altered cell-cycle profile, increased sensitivity to ɣ-irradiation and increased genomic instability, as measured using multiple approaches. To determine if these observations might mirror an *in vivo* phenotype, we also performed fluorescent *in situ* hybridization (FISH) experiments to assess genomic instability on normal breast tissue from confirmed deleterious *BRCA* carriers. Consistent with our *in vitro* observations, the archival tissue FISH results also showed an increased level of genomic copy number changes relative to wild-type *BRCA* controls. These results support the hypothesis that human breast cells hemizygous for *BRCA1* are haploinsufficient for certain BRCA1 functions, which presumably accelerates tumorigenesis in deleterious carriers (114). Since this report, other groups have provided corroborating evidence that human breast cells may be haploinsufficient for certain BRCA1 functions, namely maintenance of genomic integrity and regulation of centrosome duplication (61, 115).

From these results we reasoned that we might be able to extend our isogenic model to study other clinically reported *BRCA1* alleles for two purposes: i) develop an improved method for functional testing of *BRCA1* VUS, and ii) determine if functional differences exist between known deleterious mutations (i.e. missense versus frameshift). If validated, such a model would possess several advantages over previously developed methods. For instance, previous *in vitro* functional approaches have either studied full-length human BRCA1 within conditional *Brca1*-less embryonic mouse stem cells, studied exogenous expression of human BRCA1 in non-cancerous cells with knock-down of endogenous BRCA1 or studied exogenous expression of human BRCA1 in breast cancer cells deficient in BRCA1 (70, 107–109, 111). These approaches, although useful,

may not accurately reflect the effects different *BRCA1* mutations have on protein function, as they are either performed outside the relevant cell type and differentiation state, and/or they evaluate artificial levels of BRCA1. Assuming there is an observable phenotype for other deleterious *BRCA1* mutations (i.e. genomic instability), we posit that isogenic cell modeling would be an improvement over current *in vitro* functional approaches, since it would permit the study of different human *BRCA1* variants within an appropriate cellular context (non-cancerous human breast epithelial cells) under the normal control of the endogenous regulatory elements. Moreover, isogenic cell modeling might provide key insights into the unique phenotypes associated with specific *BRCA1* carrier states (deleterious or VUS) and the potential mechanisms that facilitate tumorigenesis amongst carriers.

For the study of VUS, we hypothesized that deleterious VUS should mimic some of the same features (e.g. increased ɣ-irradiation sensitivity and/or genomic instability) our previously derived *BRCA1*^{185delAG} isogenic derivatives exhibited. Similarly, benign VUS would be expected to behave normally in the characterization experiments. By applying this model, presumably, we might provide direct functional evidence to augment current VUS classification efforts. Secondly, we hypothesized that this approach might be suitable for detecting certain functional differences between distinct deleterious alleles. As *BRCA1* is a pleiotropic gene, involved in an array of cellular functions, it is likely that not all deleterious mutations lead to the same level of BRCA1 functional loss within cells. In other words, it is possible that not all deleterious alleles lead to the same level of haploinsufficiency. If this hypothesis holds true, if deleterious *BRCA1* alleles

demonstrate a spectrum of functionality, we may be able to stratify allele risk to improve current *BRCA1*-linked disease prevention strategies.

To test these two hypotheses, we used adeno-associated viral mediated gene targeting to genetically engineer a *BRCA1* isogenic panel within MCF-10A cells. The panel members described herein include our previously characterized *BRCA1*^{185delAG} clones, a pair of newly engineered hemizygous *BRCA1* knock-out clones (*BRCA1*$^{Ex2\text{-}3Stop}$) and eight new sets of missense mutations including, two deleterious alleles (C61G and R71G), five VUS (C64R, D67Y, L246V, S316G and Q356R) and one benign variant (I379M). Consistent with our previous work, we chose to evaluate each derivative's relative proliferation rate, ɣ-irradiation sensitivity and genomic instability. In addition, we chose to evaluate centrosome number in our derivatives, as previous functional studies have shown that BRCA1 loss of function leads to supernumerary centrosomes with aberrant multipolar mitoses (53). Furthermore, recent work suggests that mammary cells from deleterious *BRCA1* carriers may manifest *BRCA1* haploinsufficiency through elevated centrosome number, which may also contribute to genomic instability (61).

Materials & Methods

Nucleic Acid Preparation

Cell line genomic DNA (gDNA) was isolated using a QIAamp® DNA Blood Mini kit (Qiagen). All conventional Sanger sequencing of genomic DNA was carried out following PCR amplification of respective loci using Phusion® High-Fidelity DNA Polymerase (New England BioLabs). Preparation of cDNA derived RNA was performed using a First-Strand cDNA Synthesis kit (GE Healthcare).

Cell Culture

The non-tumorigenic human breast epithelial cell line MCF-10A (113) and isogenic derivatives were grown in DMEM/F12 (1:1) media supplemented with 5% horse serum (Life Technologies), 20 ng/mL epidermal growth factor (Sigma-Aldrich), 10 μg/mL insulin (Life Technologies), 0.5 μg/mL hydrocortisone (Sigma-Aldrich), 0.1 μg/mL cholera toxin (Sigma-Aldrich) and 1% Penicillin-Streptomycin (Life Technologies).

Growth Assays

Relative cell growth rates were assessed after plating 2 x 10^3 cells into 96-well plates and measuring total cellular protein using the sulforhodamine B (SRB) assay, as previously described (116). All chemicals used for the SRB assay were purchased from Sigma-Aldrich.

rAAV Construct Cloning

Details for each of the *BRCA1* alleles engineered in this study are shown in Figure 2.1A. All allelic prevalence numbers shown in Figure 2.1A were taken directly from Breast Cancer Information Core public database (updated as of January 2014), except for the artificial exon 2-3stop panel member. The *BRCA1* exon 2-3stop mutation was engineered to effectively knock out one allele of *BRCA1*, by both deleting the splice acceptor of exon 2 and replacing the start ATG with three stop codons in every reading frame (TAGaTAAcTGA). The exon 2-3stop cells and our previously described *BRCA1*^{185delAG} clones (62) were used as positive controls. All genetic manipulation of the *BRCA1* gene was carried out using distinct recombinant adeno-associated viral (rAAV) vectors for each of the three respective *BRCA1* exons shown in Figure 2.1B. Similar to our previous work (117, 118), a synthetic exon promoter trapping (SEPT) gene targeting approach was used (schematically represented in Figure 2.2A), as previously described, since this

approach greatly reduces the number of background neomycin resistant clones (119). For brevity, the representative gene-targeting scheme shown in Figure 2.2A harbors the theoretical *BRCA1* alteration in the 5' homology arm, as indicated by the asterisk. The actual mutant arms for each of the three targeting constructs are indicated in Figure 2.2B. All rAAV targeting vectors were constructed by ligating the homology arm PCR products into an adeno-associated viral plasmid (Agilent). MCF-10A gDNA was used as PCR template for each *BRCA1* targeting construct with all homology arm sizes shown in Figure 2.2B. PCR primers for homology arm construction are listed in Table 2.1. Initially, wildtype gene-targeting constructs were created for each of the respective loci listed in Figure 2.2B. Subsequently, using site-directed mutagenesis by overlap extension PCR (120) with Phusion® High-Fidelity DNA Polymerase (New England BioLabs), the wildtype targeting vectors were mutagenized to prepare each of the respective variant/mutant constructs listed in Figure 2.1A. Mutagenesis primers used to create each of the missense mutations are listed in Table 2.2.

rAAV Production

Infectious virus was prepared by co-transfecting HEK-293T cells (ATCC) with pHelper, pRC (Stratagene) and the respective *BRCA1* rAAV gene targeting plasmid. Approximately three days post-transfection, cell-free rAAV was prepared after three flash freeze/thaw cycles and filtering the growth media through a 0.22 μm filter (Millipore).

Gene Targeting of BRCA1

Gene-targeting of *BRCA1* was carried out by first transducing ~1.0 x 10^6 MCF-10A cells in 75 cm^2 tissue culture flasks and incubating for 2-3 days. Following transduction the

cells were partitioned into fourteen 96-well culture plates in the presence of G418 (Life Technologies). Following G418 selection, the gDNA of the cells were systematically pooled and screened to identify and isolate successfully targeted 'pre-Cre' neomycin resistant clones, as previously described (121). The 'pre-Cre' PCR screening primers are listed in Table 2.3. After isolation of targeted neomycin resistant 'pre-Cre' clones, the cells were then treated with Cre-expressing recombinant adenovirus and single cell diluted to obtain 'post-Cre' neomycin sensitive clones. The 'post-Cre' PCR screening primers are listed in Table 2.4. Finally, all clones were subjected to a battery of Sanger sequencing and PCR confirmation experiments to ensure each clone was monoclonal and harbored the relevant *BRCA1* alteration (Figures 2.3 and 2.4). The primers used in the confirmation experiments are shown in Tables 2.5-2.8. At least two clones were isolated for each of the engineered mutations listed in Figure 2.1A. In addition, wildtype rAAV gene targeting of both exon 5 and exon 11 was carried out to create at least one targeted wildtype control for each locus.

ɣ-Irradiation Sensitivity Assay

ɣ-irradiation sensitivity was determined by comparing sparsely seeded cells either treated with zero or six gray of radiation at a dose of approximately 3.63 gray/minute using a Xstrahl X-Ray irradiator. One day prior to ɣ-irradiation exposure, treated and untreated cells were plated in triplicate in 75 cm^2 tissue culture flasks at densities of 800 cells and 100 cells per flask, respectively. Following treatment, cells were maintained in fresh culture medium for 8-10 days until colonies were readily visible. For colony counting, cells were fixed and stained with 3.7% formaldehyde containing 0.2% (wt/vol) Crystal

violet (Sigma-Aldrich). Relative radio-sensitivity was defined as the inverse of fractional survival, as shown in Figure 2.6A.

Fluorescent in situ Hybridization

For all fluorescent *in situ* hybridization experiments, 1.0 x 10^5 cells were plated in 8-well BD Falcon™ glass chamber slides (Fisher Scientific) and grown exponentially for two days before being fixed with 10% neutral buffered formalin (Sigma-Aldrich). Following fixation, cells were washed in phosphate buffered saline (PBS) pH 7.4 (Life Technologies) and treated with a FISH pretreatment reagent kit (Abbott Molecular), according to the manufacturer's recommendations. Pretreated, dehydrated slides were then probed simultaneously with Vysis LSI *RET* (Tel) SpectrumOrange and Vysis LSI *MYC* SpectrumGreen gene probes (Abbott Molecular). Following probe hybridization, slides were counterstained with 0.5 μg/mL 4,6-diamidino-2-phenylindole (DAPI) for 5 minutes and mounted with Prolong Gold (Sigma-Aldrich and Life Technologies, respectively). Using a Nikon Eclipse 50i fluorescent microscope, at least 200 interphase cells were observed for gene copy number gains and losses. Percent copy number (CN) change from the mode was determined as the percentage of cells whose copy number deviated from the modal population for each gene probe. All derivatives harbored a *MYC* modal copy number of three and a *RET* modal copy number of two. To control for experimental variability across multiple experiments, each independent experiment included parental MCF-10A alongside each engineered derivative. Therefore, all data is reported as relative to parental MCF-10A.

Immunofluorescence

To assess centrosome number in MCF-10A cells and all engineered derivatives, 1.0 x 10^5 cells were plated in chamber slides and grown for two days under exponential growth conditions, before being fixed in cold methanol for 15 minutes at -20°C. Following fixation, cells were washed with cold acetone and treated for two hours with PBS containing 5% goat serum and 0.3% Triton X-100 (Sigma-Aldrich). A primary rabbit antibody against ɣ-tubulin was applied to the cells (Sigma-Aldrich) for one hour followed by a secondary goat anti-rabbit antibody conjugated to Alexa488 (Life Technologies) for 20 minutes. The plasma membrane was stained with 5 μg/mL Texas Red®-X conjugated wheat germ agglutinin (WGA) for five minutes (Life Technologies) and the nucleus was counterstained with 0.5 μg/mL 4',6-diamidino-2-phenylindole (DAPI) for one minute (Sigma-Aldrich). The percentage of cells with greater than two centrosomes was determined by viewing at least 200 cells for each panel member using a Nikon Eclipse 50i fluorescent microscope. Similar to the FISH analyses described above, each independent experiment included parental MCF-10A alongside each engineered derivative. Therefore, all data is reported as relative to parental MCF-10A.

Ploidy Estimation

Ploidy estimation was carried out by analyzing cells stained with the DNA intercalating agent, propidium iodide. Initially, 5.0 x 10^5 cells were grown under exponential growth conditions for two days before being trypsinized, washed with cold PBS and fixed with 70% cold ethanol. Fixed cells, stored for 1-7 days at -20°C, were then washed once with cold PBS before being stained with 40 μg/mL propidium iodide (Sigma-Aldrich) in the presence of 500 μg/mL DNase-free RNase A (Sigma-Aldrich) in 0.1% Triton X-100 (Sigma-Aldrich) in PBS at 37°C for 15 minutes. For each isogenic derivative, at least

10,000 cells were analyzed using a FACSCalibur™ (BD Biosciences) for cell cycle distribution and polyploidy (>4n). To account for potential clonal artifacts, all data was normalized to parental MCF-10A and compared to targeted wild type controls.

Statistical Considerations

All statistical analyses were carried out using GraphPad Prism 6 software with *P* value significant level indicated using one or more asterisks: $P \leq 0.05$ (*),$P \leq 0.01$ (**) and $P \leq 0.001$ (***). Relative proliferation rates were analyzed by two-way ANOVA. Relative radiosensitivies were compared to both parental MCF-10A and controls using unpaired t-tests. Results from the FISH, immunofluorescence and cell-cycle experiments were compared to control samples using unpaired t-tests.

Results

Engineering an Isogenic BRCA1 Panel

To perform *in vitro* modeling of different *BRCA1* carrier states, gene targeting experiments were conducted in the human non-tumorigenic breast epithelial cell line, MCF-10A (113). Figure 2.1 lists each of the engineered *BRCA1* alleles, their recorded prevalence, clinical designation and respective locus. In each gene targeting experiment, at least two independently derived clones were isolated for each of the respective mutations/variants. In each of the described assays, the presented data represents means across ≥2 clones for each genetically distinct panel member. To control for clonal variation and/or possible effects caused by the gene targeting process, three independent targeted wild-type clones (two for exon 5 and one for exon 11) were established. For clarity, data generated for all three targeted wild-type control clones were grouped

together, as they all are expected to behave similarly. To act as positive controls in the characterization experiments, two unique pairs of BRCA1 truncating clones were used: our previously described *BRCA1*^{185delAG} cells and our newly established *BRCA1*$^{Ex2\text{-}3stop}$ clones (described in the Materials & Methods).

For VUS modeling, we engineered five different VUS derivatives. The *BRCA1*^{C64R} derivative harbors a missense mutation located at the C-terminal end of BRCA1's N-terminally located RING domain. The C64 residue is the last of several conserved zinc-coordinating residues located in the RING domain of BRCA1. Despite several studies describing the C64G missense mutation as deleterious, it remains unclear whether the C64R mutation is deleterious (70, 111, 122). The D67Y mutation lies adjacent to BRCA1's RING domain and its clinical significance remains controversial. Currently, the BIC catalogs the D67Y mutation as a VUS, however, a large probabilistic study in 2007 classified it as benign (123). In contrast, some functional data exists suggesting that the D67Y may be hypomorphic, affecting BRCA1's E3 ubiquitin ligase activity, and as a result, potentially centrosome dynamics and cisplatin sensitivity (108, 124). The three other VUS derivatives engineered in this study, *BRCA1*^{L246V}, *BRCA1*^{S316G} and *BRCA1*^{Q356R}, map to a region purported to bind several important transcriptional factors, including c-MYC, TP53, RB and RAD50 (125–129). In addition, we engineered a benign variant located within the same region, *BRCA1*^{I379M}, to better evaluate the validity of our model.

To evaluate potential functional differences between deleterious mutations, we engineered two additional deleterious derivatives, *BRCA1*^{C61G} and *BRCA1*^{R71G}. The RING domain mutation, *BRCA1*^{C61G}, is the third most commonly reported deleterious

BRCA1 mutation, according to the BIC, and is thought to disrupt normal quaternary structure of the BRCA1/BARD1 heterodimer (37). The *BRCA1*^{R71G} mutation is a deleterious Spanish founder mutation that leads to aberrant splicing (130).

Truncating BRCA1 Mutations Confer Slowed Proliferation

First, we chose to study the proliferation rates of each of the *BRCA1* panel members, since in our previous work we found that cells harboring the *BRCA1*^{185delAG} allele demonstrate slowed proliferation, as compared to parental MCF-10A cells. Mean relative growth rates are shown in Figure 2.5. In accord with previous observations, cells harboring a truncating allele, either *BRCA1*$^{Ex2\text{-}3stop}$ or *BRCA1*^{185delAG} cells, grew significantly slower than parental MCF-10A and controls. In contrast, cells harboring the deleterious missense mutation, *BRCA1*^{R71G}, grew similar to controls. The *BRCA1*^{C61G} clones grew slightly slower than MCF-10A and controls. These results suggest that deleterious missense mutations may not be functionally synonymous with deleterious truncating mutations. The three VUS, *BRCA1*^{C64R}, *BRCA1*^{D67Y}, *BRCA1*^{Q356R}, appeared to have not significant change in growth kinetics, whereas the *BRCA1*^{L246V}and *BRCA1*^{S316G} derivatives did demonstrate slowed growth. These results suggest that the *BRCA1*^{L246V}and *BRCA1*^{S316G} mutations may have an effect on normal BRCA1 function. Lastly, the *BRCA1*^{I379M} benign variant cells grew marginally slower than parental MCF-10A, but similar to its targeted wild-type control.

Specific BRCA1 Genotypes Confer Sensitivity to ɣ*-irradiation*

Next, we went on to assay each panel member's sensitivity to ɣ-irradiation at 6 gray. Mean relative radio-sensitivities are shown in Figure 2.6B. Again, consistent with

previous work, cells harboring one truncating *BRCA1* allele demonstrated a statistically significant increase in sensitivity to ionizing radiation. Notably, the *BRCA1*^{185delAG} cells demonstrated the largest radio-sensitivity across all deleterious clones, suggesting this mutation is uniquely deleterious. In addition, the *BRCA1*^{C61G}, *BRCA1*^{R71G}, *BRCA1*^{C64R} and *BRCA1*^{Q356R} clones also demonstrated increased sensitivity to ionizing radiation. Similar to the relative change in proliferation rates, the missense deleterious clones did not demonstrate as severe ɣ-irradiation sensitivity as the deleterious truncating clones, again suggesting a spectrum of functionality exists amongst deleterious alleles. The *BRCA1*^{C64R} VUS demonstrated radio-sensitivity similar to the *BRCA1*^{C61G} clones, suggesting this variant is deleterious. And lastly, the *BRCA1*^{Q356R} variant demonstrated a small increase in radio-sensitivity, suggesting this allele might also be hypomorphic. As expected, cell harboring the *BRCA1*^{I379M} benign variant were not more radiosensitive than controls.

Chromosomal Instability (CIN)

To assess chromosomal instability (CIN), we chose to use the conventional method of fluorescent *in situ* hybridization (FISH). FISH permits investigators to not only observe a cell's genomic state (i.e. copy number), but also the frequency of copy number deviation across many cells within a given cell population; or CIN (131). For all panel members, we evaluated CIN using two gene probes (*MYC* and *RET*). CIN estimates are reported as the average relative copy number deviation for each probe and are shown in Figure 2.7. As expected, cells harboring a truncating *BRCA1* allele demonstrated an increase in CIN for both gene probes tested. Interestingly, the two sets of missense deleterious clones, *BRCA1*^{C61G} and *BRCA1*^{R71G}, also demonstrated CIN, but only for the *RET* gene probe.

These results further suggest that not all deleterious *BRCA1* mutations are functionally equivalent.

The *BRCA1*^{C64R} and *BRCA1*^{D67Y} VUS were the only other derivatives demonstrating statistically significant CIN. Consistent with the irradiation experiments, these results suggest that the *BRCA1*^{C64R} VUS is a deleterious variant. Although the *BRCA1*^{D67Y} cells did demonstrate statistically significant CIN, the difference from controls was relatively small. In accord with other work, these results suggest that the *BRCA1*^{D67Y} allele may have hypomorphic properties. As expected, cell harboring the *BRCA1*^{I379M} variant did not demonstrate CIN, further corroborating its neutral effect on protein function.

Cell-Cycle Analysis Reveals an Increased Fraction of Polyploid Cells

During the FISH experiments described above, we also observed a striking trend; many (but not all) of the clones demonstrating CIN appeared to display a small but observable fraction of cells with >2 times the modal copy number for one or both gene probes, as shown in Figure 2.8A. This led us to perform cell cycle analysis for ploidy estimation. Figure 2.8B shows the average percentage of cells with >4n for each derivative normalized to parental MCF-10A. Interestingly, the deleterious missense mutants, *BRCA1*^{C61G} and *BRCA1*^{R71G}, both demonstrated a larger fraction of polyploid cells, but the truncating mutants did not. Again, these results suggest that not all deleterious mutations are functionally synonymous. Additionally, two VUS, *BRCA1*^{D67Y} and *BRCA1*^{S316G}, appeared to demonstrate a statistically significant increase in polyploid events. These results suggest that the *BRCA1*^{D67Y} variant does abrogate normal BRCA1

function. As expected, the *BRCA1*^{I379M} derivatives demonstrated results very similar to controls, suggesting this neutral variant has no impact on normal BRCA1 function.

Centrosome Amplification

Lastly, BRCA1 has been implicated in the regulation of centrosome duplication, whereby inhibition of BRCA1 or loss of function leads to an increase in cell centrosome number (74). Interestingly, a recent study showed that normal breast tissue from deleterious *BRCA1* carriers displays increased centrosome number, relative to controls (61). The abnormal centrosome dynamics observed in BRCA1-altered cells appears to be linked to the functionality conferred by BRCA1's RING domain, where the *BRCA1*^{C61G} and *BRCA1*^{C64R} mutations localize (55, 74, 108).

Therefore, to study whether our isogenic panel members also demonstrate an increase in overall centrosome number, we performed immunofluorescent staining of ɣ-tubulin, a major centrosomal core protein, to quantify cellular centrosomes. Relative centrosome amplification results with representative images are shown in Figure 2.9. In line with the observations made by Martins et al., we observed an increase in centrosome number for cells harboring a deleterious allele, namely the *BRCA1*^{185delAG}, *BRCA1*$^{exon\ 2\text{-}3stop}$ and *BRCA1*^{R71G} derivatives. Unexpectedly, the *BRCA1*^{C61G} cells did not demonstrate a significant increase in centrosome number relative to parental MCF-10A or controls. It is possible that truncating *BRCA1* mutations have a larger effect on centrosome number than *BRCA1* RING mutants. This is consistent with the similar results observed for the *BRCA1*^{C64R} variant. However, the *BRCA1*^{C64R} variant did demonstrate statistically significant change. Nonetheless, these results further suggest that the *BRCA1*^{C64R} variant is deleterious. The *BRCA1*^{D67Y} variant demonstrated the highest number of multi-polar

mitoses among all panel members, again suggesting this variant does influence function. Interestingly, the centrosome amplification observed for the *BRCA1*^{D67Y} cells appears to correlate with the fraction of polyploidy cells discussed above.

Table 2.9 summarizes the results across all of the characterization assays described above.

Table 2.1: Homology Arm Cloning Primers

Locus	Homology Arm	Forward/Reverse
Exon 2 (3Stop)	5’	5’-TCGTATTCTGAGAGGCTGCTGCT 5’-TCACATATTGCTGCCAACCC
	3’	5’-GCTCTTCGCGTTGAAGAAGTAC 5’-GCCAGTTTCAAACAAAGGTTCTTCC
Exon 5	5’	5’-CGCTTGATCACAGATGTATG 5’-CCAACCTAGCATCATTACCA
	3’	5’-AAGCAACCACAGTAGGAAAAAGTAG 5’-CTCGTACTTTCTTGTAGGCTC
Exon 11 (5’)	5’	5’-GAAATCAGTTTGGATTCTGCA 5’-TGGAAATCAACCAACTGGCT
	3’	5’-CCTCCAAGGTGTATGAAGTATG 5’-GGTTAGTTCCCTGATTTATCATTTC

Table 2.2: Mutagenesis Primers

Locus	Variant/Mutant	Forward/Reverse
Exon 5	C61G	5’-GGGCCTTCACAGgGTCCTTTATGTAAG 5’-CTTACATAAAGGACcCTGTGAAGGCCC
	C64R	5’-CAGTGTCCTTTACGTAAGAATGAT 5’-ATCATTCTTACGTAAAGGACACTG
	D67Y	5’-TATGTAAGAATtATATAACCAAAAGGT 5’-ACCTTTTGGTTATATaATTCTTACATA
	R71G	5’-GATATAACCAAAgGGTATATAATTTGG 5’-CCAAATTATATACCcTTTGGTTATATC
Exon 11 (5’)	L246V	5’-CAGTAATAATGATgTGAACACCACTGAG 5’-CTCAGTGGTGTTCAcATCATTATTACTG
	S316G	5’-CTTAGCAAGGgGCCAACATAAC 5’-GTTATGTTGGCcCCTTGCTAAG
	Q356R	5’-GAATGGAATAAGCgGAAACTGCCATGCTC 5’-GAGCATGGCAGTTTCcGCTTATTCCATTC
	I379M	5’-CTAAATAGCAGCATgCAGAAAGTTAATGAG 5’-CTCATTAACTTTCTGcATGCTGCTATTTAG

Table 2.3: Pre-Cre Screening Primers

Locus	Homology Arm	Forward/Reverse
Exon 2 (3Stop)	5’	5’-GACCTCTTCTTACGACTGCTTTG 5’-ATGTATGCTATACGAAGTTATGGATCC
	3’	5’-TTAAGGTACCACTGTGCATATG 5’-CCAGCCTCTCGACAGAGATC
Exon 5	5’	5’-GACCATCCTGGCTAACATGG 5’-CATTGTCACTCAAGTGTATGGC
	3’	5’-TTAAGGTACCACTGTGCATATG 5’-CTCCAAACCTGTGTCAAGCTG
Exon 11 (5’)	5’	5’-GACAGTTCTGCATACATGTAACTAG 5’-GCAGACAGCGAATTAATTCC
	3’	5’-TTAAGGTACCACTGTGCATATG 5’-CGAGTGATTCTATTGGGTTAGG

Table 2.4: Post-Cre Screening Primers

Locus	Forward/Reverse
Exon 2 (3Stop)	5’-GACCTCTTCTTACGACTGCTTTG 5’-CATATGCACAGTGGTACCTTAA
Exon 5	5’-ACTAGTGGATCCATAACTTCG 5’-CTCCAAACCTGTGTCAAGCTG
Exon 11 (5’)	5’-GACAGTTCTGCATACATGTAACTAG 5’-CATATGCACAGTGGTACCTTAA

Table 2.5: PCR Primers Across *loxP* Scar

Locus	Forward/Reverse
Exon 2 (3Stop)	5'-GGAGAAAGCTAAGGCTACC
	5'-AGTGGATGGAGAACAAGGAA
Exon 5	5'-CTTAAGGGCAGTTGTGAGATTATC
	5'-CCTGTATAAGGCAGATGTCC
Exon 11 (5')	5'-CACTCTTAGACGTTAGAG
	5'-CAAAAATAACAAGGTACTCAA

Table 2.6: Targeted Allele Sequencing Primers

Locus	Forward/Reverse	Nested
Exon 2 (3Stop)	5'-GACCTCTTCTTACGACTGCTTTG	5'-GGAGAAAGCTAAGGCTACC
	5'-CATATGCACAGTGGTACCTTAA	
Exon 5	5'-GACCATCCTGGCTAACATGG	5'-CTTAAGGGCAGTTGTGAGATTATC
	5'-ATGTATGCTATACGAAGTTATGGATCC	
Exon 11 (5')	5'-TTAAGGTACCACTGTGCATATG	5'-TATATTTTCAGCTGCTTGTGAAT
	5'-CGAGTGATTCTATTGGGTTAGG	

Table 2.7: Bi-Allelic Sequencing Primers

Locus	Forward/Reverse	Nested
Exon 5	5'-ATTTCTGTACTGTCAATTCC 5'-CCAACCTAGCATCATTACCA	5'-CTTAAGGGCAGTTGTGAGATTATC
Exon 11 (5')	5'-CCTCCAAGGTGTATGAAGTATG 5'-CCTAACAGTTCATCACTTCTGG	5'-TATATTTTCAGCTGCTTGTGAAT

Table 2.8: cDNA Sequencing Primers

Locus	Forward/Reverse	Nested
Exon 5	5'-AGCTCGCTGAGACTTCCTG 5'-GGAACATCTTCAGTATCTCTAGG	5'-GCCCATACTTTGGATGATAG
Exon 11 (5')	5'-CCTTGGAACTGTGAGAACTCTG 5'-CGAGTGATTCTATTGGGTTAGG	5'-CTGCTTGTGAATTTTCTGAGAC

Table 2.9: Isogenic Panel Summary

ID	Radiosensitive	Chromosomal Instability		Increased Polyploid Fraction	Centrosome Amplification	Current Clinical Designation
		MYC	RET			
Ex2-3Stop	+	+	+	-	+	N/A
185delAG	+	+	+	-	+	Deleterious
R71G	+	-	+	+	+	Deleterious
C61G	+	-	+	+	-	Deleterious
C64R	+	-	+	-	+	VUS
D67Y	-	-	+	+	+	VUS
S316G	-	-	-	+	-	VUS
Q356R	+	-	-	-	-	VUS
L246V	-	-	-	-	-	VUS
I379M	-	-	-	-	-	Benign

A

Exon	Alteration	Base Change	Prevalence	Clinical Classification
2	Ex2-3Stop	-	Artificial	Artificial Deleterious
	185delAG	c.66_67delAG	1988	Deleterious
5	C61G	c.181T>G	230	Deleterious
	C64R	c.190T>C	12	VUS
	D67Y	c.199G>T	8	VUS
	R71G	c.211A>G	35	Deleterious
11 (5')	L246V	c.736T>G	80	VUS
	S316G	c.946A>G	6	VUS
	Q356R	c.1067A>G	155	VUS
	I379M	c.1137T>G	24	Benign

B

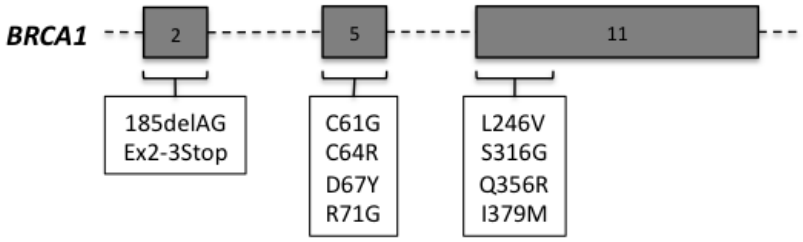

Figure 2.1: Overview of the *BRCA1* alleles genetically engineered in this study. A) Table showing genomic locus, prevalence and current designation for each introduced allele. The prevalence represents the number of unique entries cataloged into the the Breast Cancer Information Core (BIC), as of January 2014. The current clinical classification of each allele is also taken directly from the BIC. B) Schematic representation of each exon targeted in this study (not drawn to scale).

A

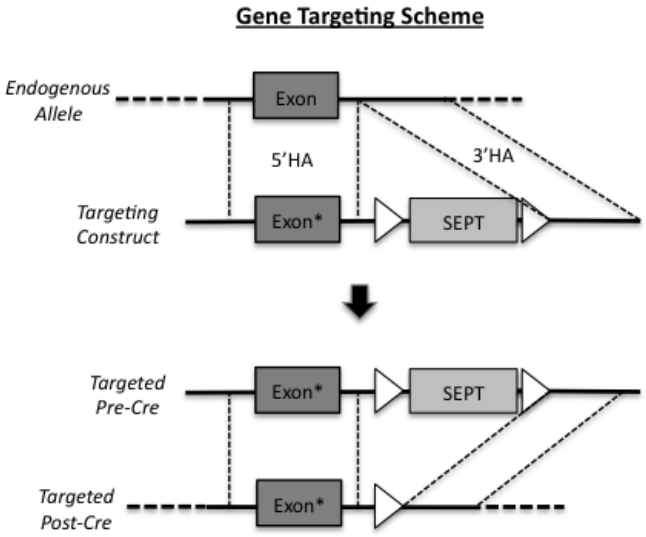

B

	Targeting Construct Specifications		
Exon	**5'HA (bp)**	**3'HA (bp)**	**Mutant Arm**
2	1150	759	3'
5	608	1490	5'
11 (5')	934	1021	3'

Figure 2.2: Gene targeting overview. A) Representative rAAV-mediated gene targeting schematic for a targeting vector with an exonic mutation (denoted by the asterisk) within the 5' homology arm (HA). First, rAAV transduction facilitates integration of the targeting vector via homologous recombination between the 5' and 3'HAs. Following neomycin selection and clone isolation, the *loxP* flanked (white triangle) SEPT cassette is excised using Cre recombinase, leaving only a small intronic *loxP* scar. B) Table showing both the homology arm sizes and the respective mutant arm for each of the gene targeting constructs used in this study.

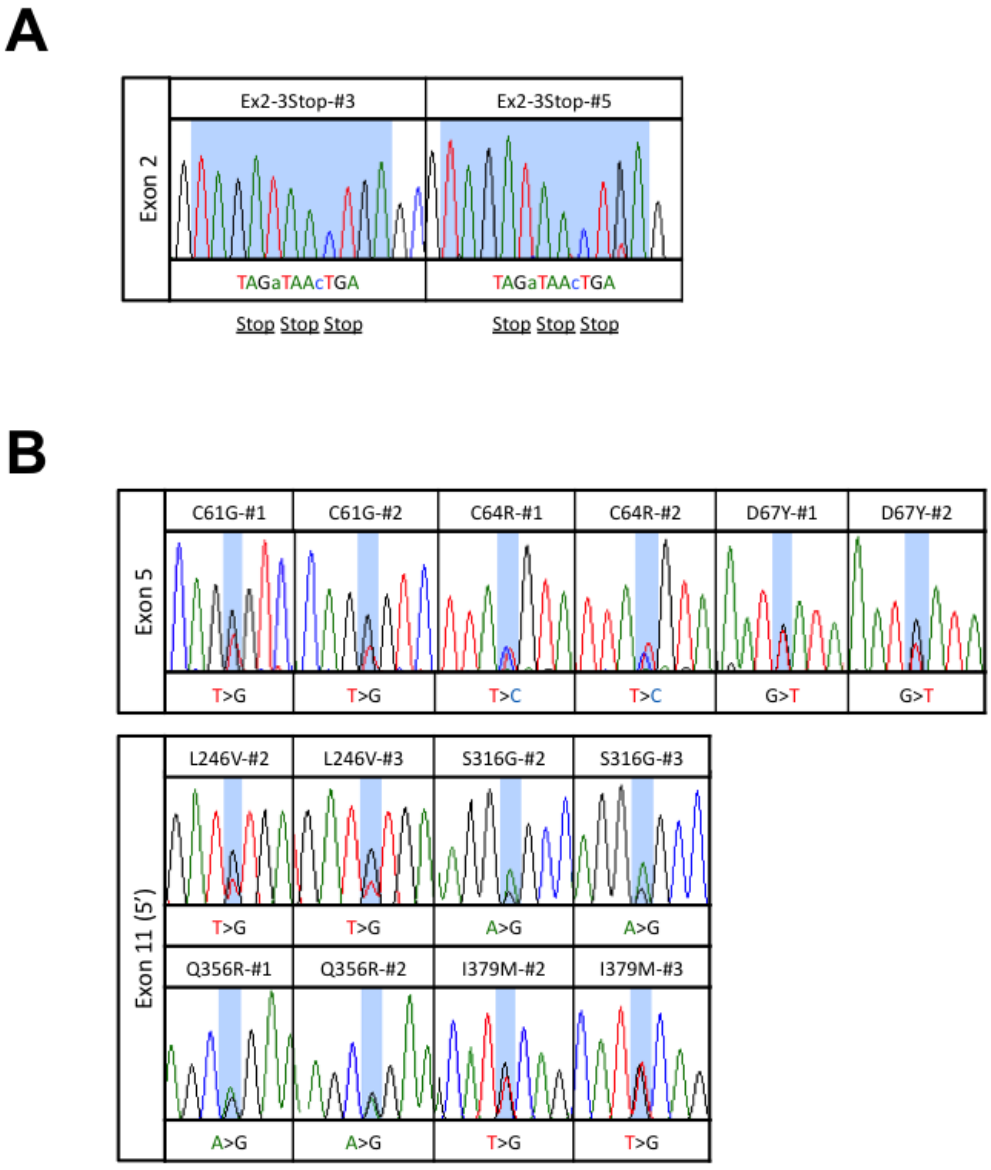

Figure 2.3: Sanger sequence traces for the engineered *BRCA1* panel members. A) gDNA sequences for the two exon 2-3stop hemizygous knock-out clones. B) cDNA sequences for the exon 5 and exon 11 clones. The R71G clones are not shown, as this mutation disrupts normal splicing.

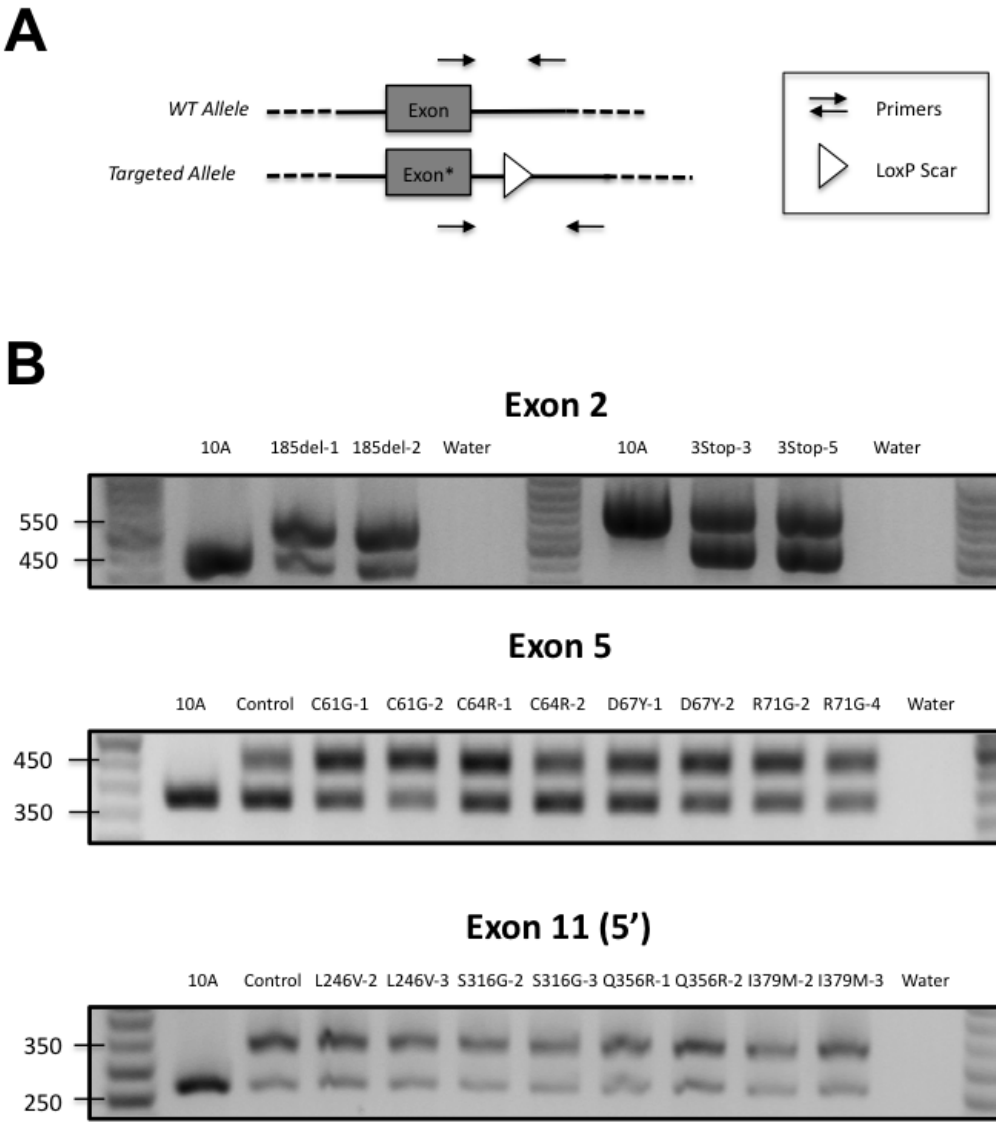

Figure 2.4: Genetic confirmation of isogenic panel members via PCR analysis. A) Schematic of PCR using loxP scar spanning genomic primers. As shown, PCR of the targeted allele generates a larger PCR amplicon. B) 2% agarose gel with PCR products for each of the three loci gene targeted.

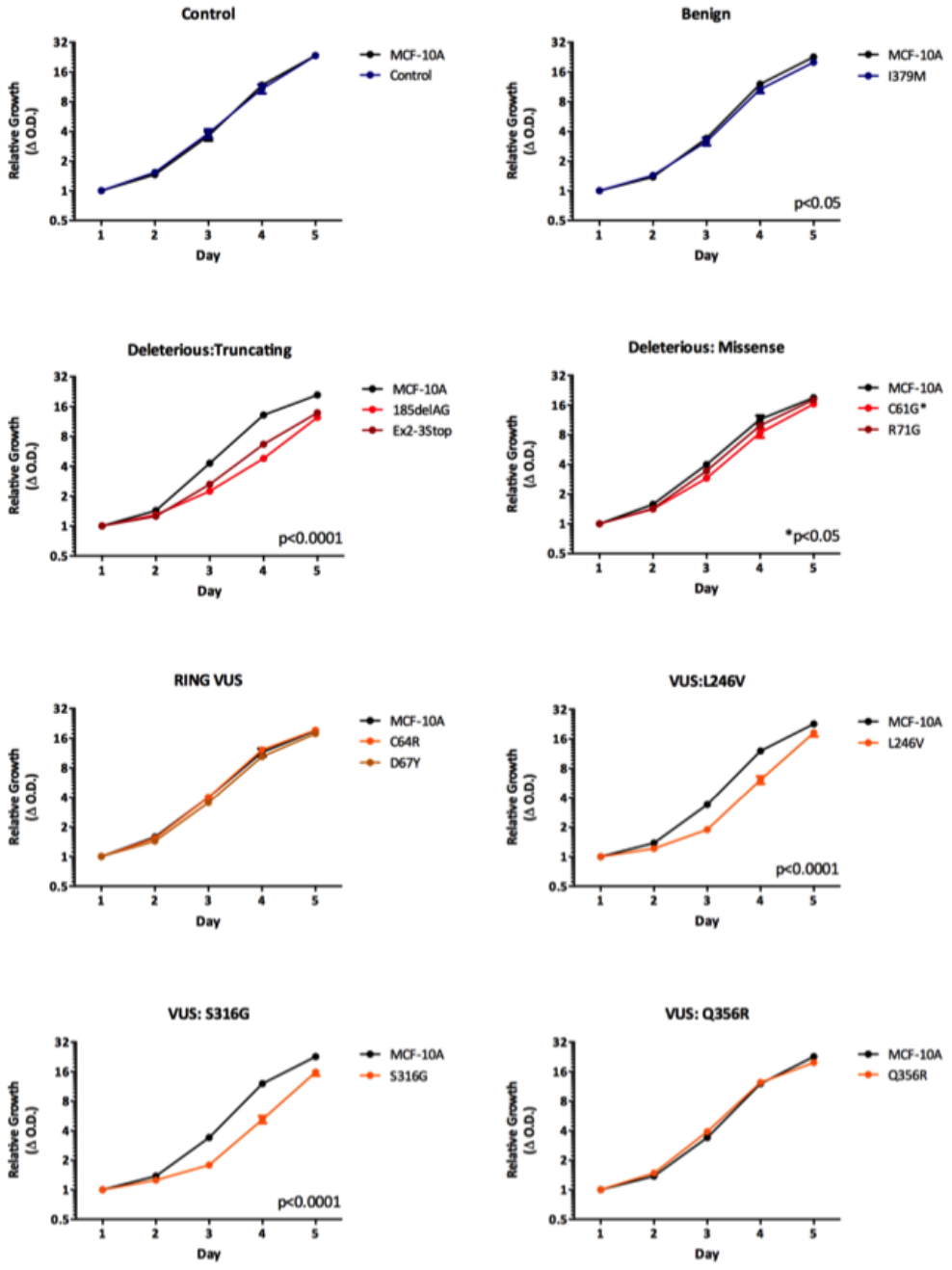

Figure 2.5: Mean relative proliferation rates for all isogenic panel members, as measured by the SRB assay (error = SEM). Values represent means across at least two clones per mutation with each assayed at least in triplicate. Clones demonstrating significantly different growth rates are indicated.

A

$$\text{Relative Radiosensitivity} = \frac{1}{x} \qquad \text{where } x = \frac{\left[\frac{\#\text{ treated colonies}}{\#\text{ untreated colonies}}\right]}{\text{plating factor}}$$

B

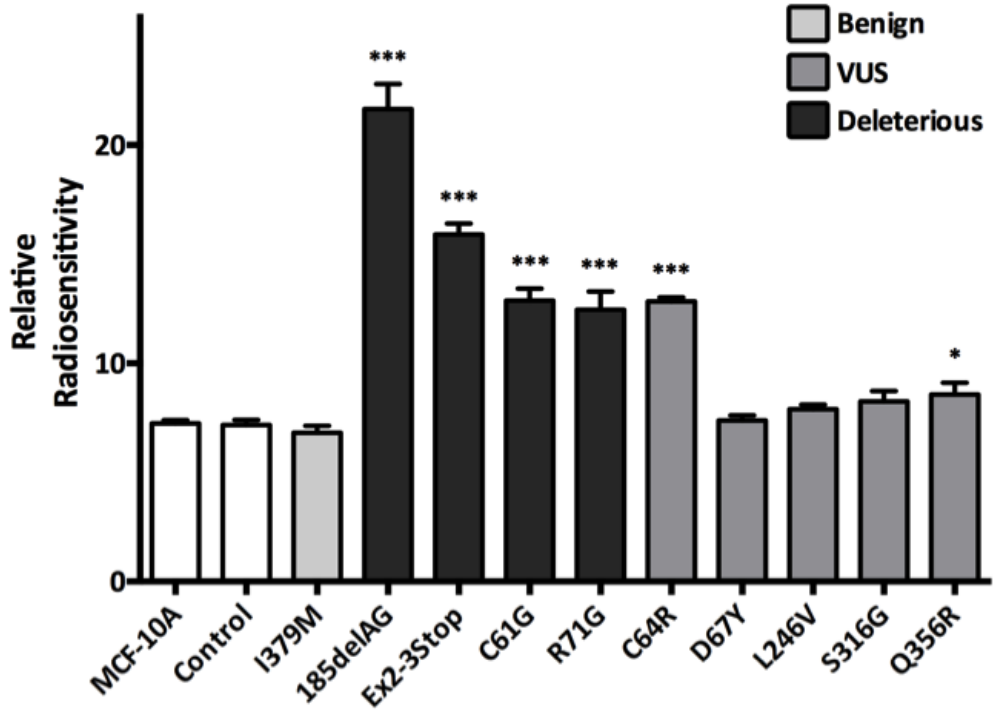

Figure 2.6: Mean relative radiosensitivities for all panel members at 6 gray γ-irradiation. A) Definition of relative radiosensitivity. *Note*, plating factor = 8 (800 cells plated for 6 gray and 100 cells plated for 0 gray). B) Bar graphs showing mean relative radiosensitivity (error = SEM) for at least two clones per mutation with each assayed at least in triplicate. Clones demonstrating statistically significant increases in radiosensitivity, relative to MCF-10A and controls, are indicated by the asterisks.

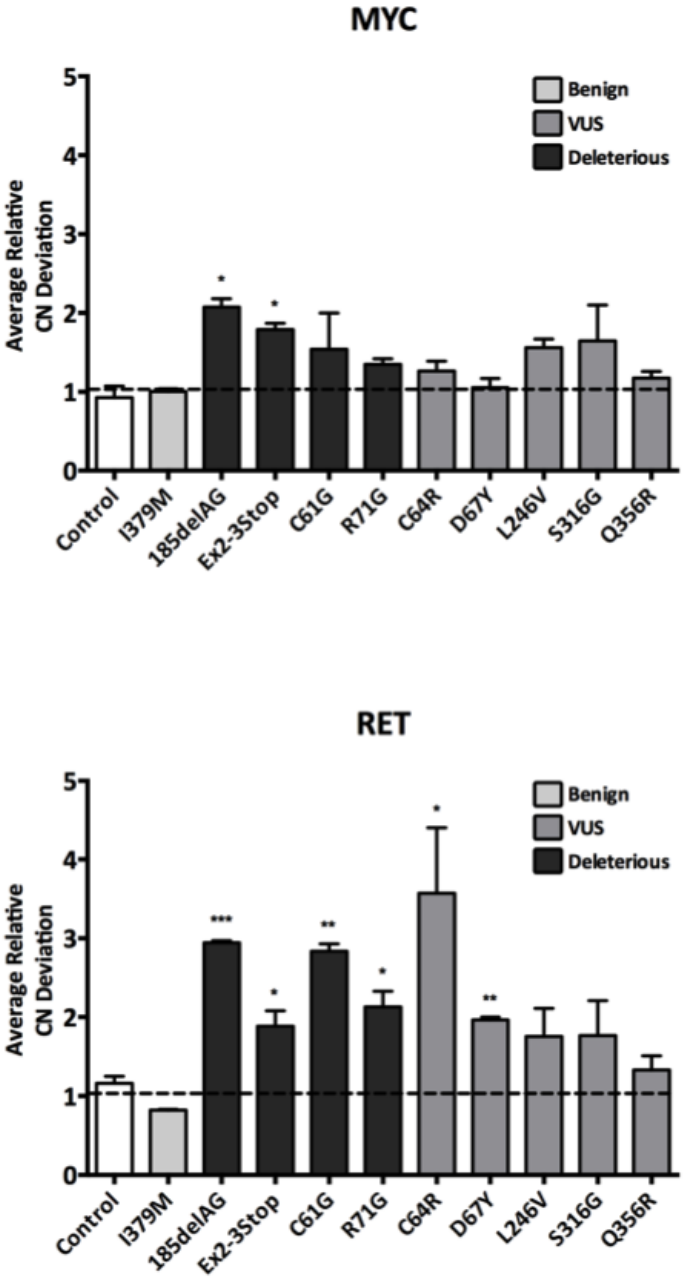

Figure 2.7: Chromosomal instability (CIN) as measured by fluorescent *in situ* hybridization (FISH). Histograms display average copy number (CN) deviations, relative to parental MCF-10A, for all panel members using the MYC and RET gene probes (error = SEM). Isogenic derivatives demonstrating statistically significant differences are indicated.

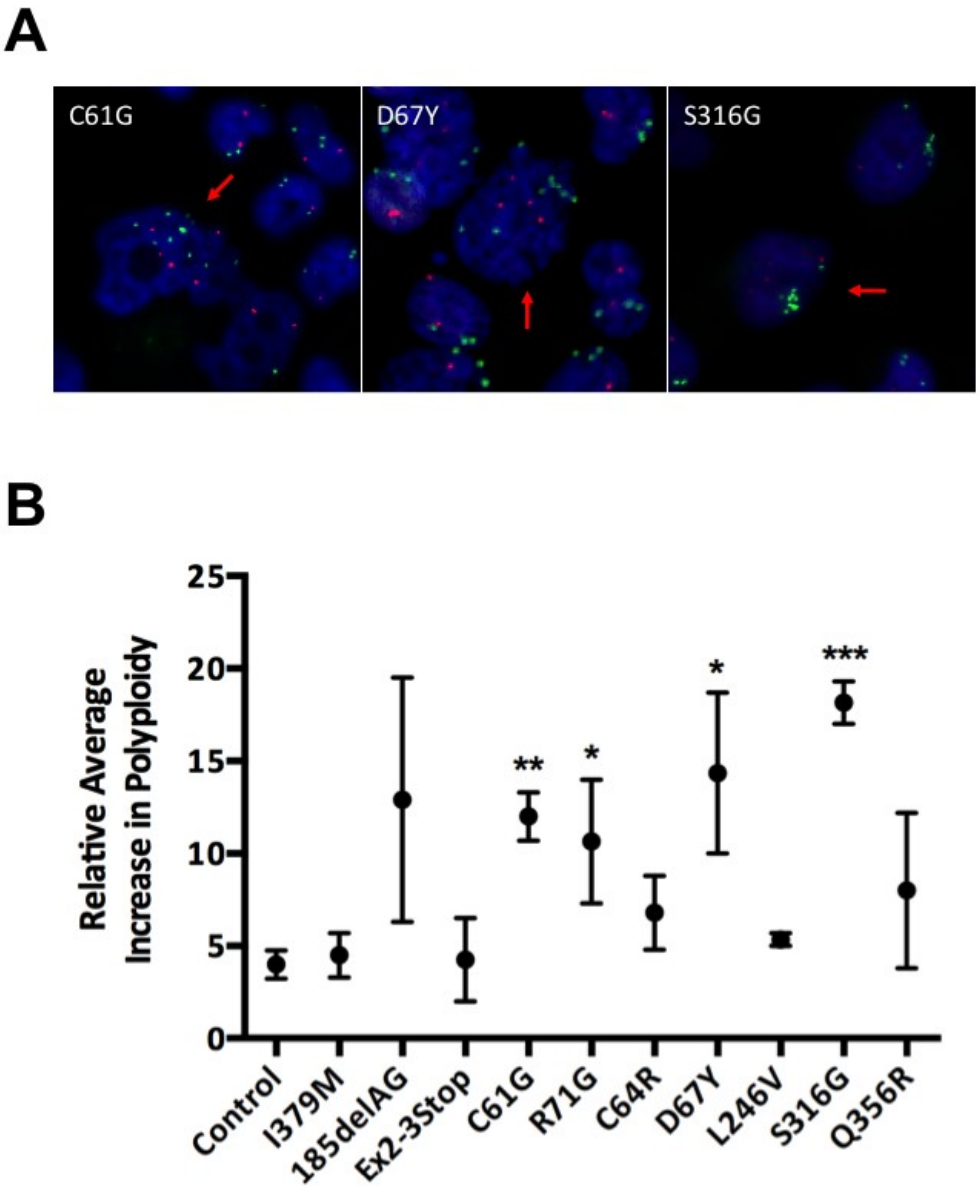

Figure 2.8: Ploidy estimation. A) Representative FISH images for derivatives demonstrating large abnormally shaped nuclei with >2x the modal copy number for MYC and/or RET genes, indicated by the red arrows. B) Scatter plot showing the average increase in the percent observed polyploidies relative to parental MCF-10A (error = SEM), across at least two clones for each. Isogenic derivatives demonstrating statistically significant increases are indicated.

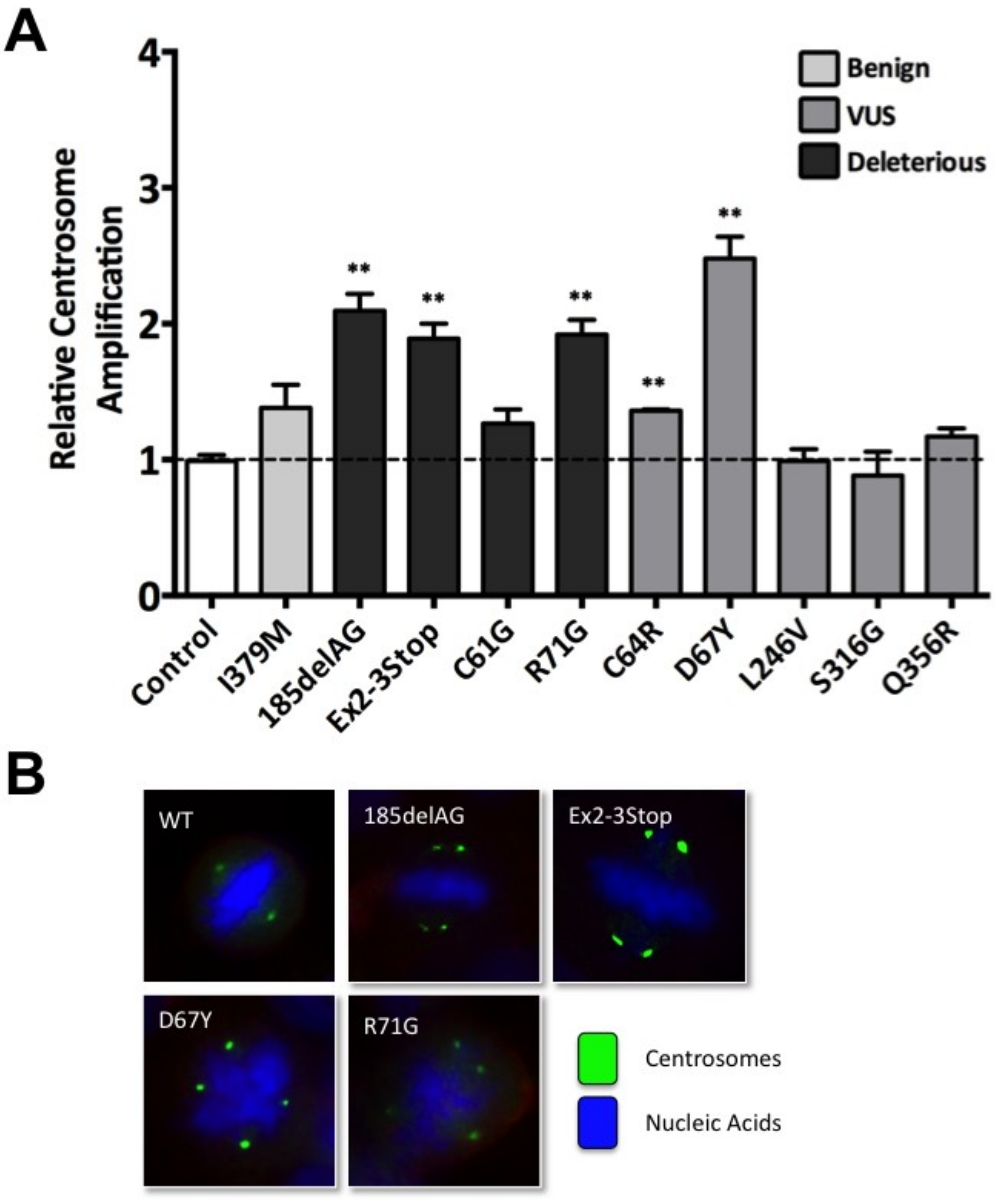

Figure 2.9: Relative centrosome amplification. A) Average centrosome amplification relative to parental MCF-10A for all panel members (error = SEM). Isogenic derivatives demonstrating statistically significant amplification, relative to controls, are indicated. B) Representative images for cells demonstrating multipolar mitoses due to aberrant centrosome number. Green represents immunofluorescent staining of γ-tubulin, blue identifies nucleic acids (DAPI) and red identifies the plasma membrane.

3 Droplet digital PCR for *BRCA* LOH Analysis

Introduction

Loss-of-heterozygosity (LOH) analysis of resected tumor tissue has been helpful for classifying particular *BRCA* VUS (105, 132–134). Yet several technical hurdles exist that hinder archival tissue-based studies. In particular, formalin fixation leads to a high degree of tissue damage, yielding a limited amount of usable DNA molecules for downstream applications. Moreover, contaminating normal DNA present within formalin fixed paraffin embedded (FFPE) tumor DNA preparations can hinder many genetic analyses. Additionally, techniques such as fluorescence *in situ* hybridization (FISH) have intrinsic shortcomings that make analysis of archival tissue challenging. Specifically, FISH is subjective, prone to inter-observer variability, has limited sensitivity, can be technically difficult, time consuming, and cannot identify certain genomic alterations, such as loss with duplication (135). To circumvent some of these challenges and facilitate future LOH studies, droplet digital PCR (ddPCR) was used to study genomic DNA derived from

archival tumor tissues from two members of a cancer prone family harboring a *BRCA2* VUS.

Materials & Methods

Combined Clinical History

A 46-year-old woman of non-Ashkenazi ancestry and a family history of cancer, presented to the clinic for genetic counseling and testing for hereditary breast and ovarian cancer syndromes. Three years prior to her presentation, the proband was diagnosed with a grade II invasive ductal carcinoma (IDC) of the right breast with ductal carcinoma *in situ* (DCIS). The proband's tumor was found to co-express estrogen and progesterone receptors (ER^+/PR^+), and did not over-express the human epidermal growth factor receptor 2 ($HER2^-$). The proband's mother was also diagnosed with a grade I IDC of the left breast with DCIS at the age of 76. Following a consultation with the proband, she and her mother were encouraged to pursue germline testing for mutations/alterations of the *BRCA1* and *BRCA2* genes. Clinical genetic testing for the proband and her mother revealed the presence of a *BRCA2* variant of uncertain clinical significance (c.6966G>T; M2322I).

Tissue Processing, Nucleic Acid Preparation & Sanger Sequencing

Buccal and FFPE derived genomic DNA (gDNA) was isolated using QIAamp® DNA Blood Mini and QIAamp® FFPE tissue kits, respectively (Qiagen, Valencia, CA). Genomic DNA was isolated from FFPE tissue using standard protocols. Briefly, H&E stained histology slides were examined by a pathologist to identify areas of at least 70% breast carcinoma cells and adjacent benign lobular epithelial cells with 0% tumor cells greater than 10mm from any invasive component,

hereafter termed FFPE tumor and FFPE normal, respectively. Five-micron thick unstained slides were deparaffinized and identified regions of interest were macrodissected using the Zymo pen and Pinpoint solution (Zymo Research, Irvine, CA), per the manufacturer's protocol. Sanger sequencing of gDNA was carried out following PCR amplification of respective loci using Phusion® High-Fidelity DNA Polymerase (New England BioLabs, Ipswich MA). PCR and nested sequencing primers for each locus described herein are listed in Table 3.1.

Droplet Digital PCR Experiments

All droplet digital PCR experiments were carried out using the QX100™ Droplet Digital PCR System according to the manufacturer's protocols (Bio-Rad, Hercules, CA), as previously described (136). Droplet Digital PCR primers were purchased from Integrated DNA Technologies (Coralville, IA) and fluorescently labeled TaqMan® probes were purchased through Life Technologies (Carlsbad, CA). Primer and probe sequences are shown in Table 3.2. Prior to analysis of patient DNA samples, optimized thermo-cycling conditions were determined for allele-specific binding of the fluorescent probes by initially cloning 381 base pairs of genomic sequence encompassing *BRCA2* exon 13 (both the wild-type and VUS alleles) with flanking intronic sequence into a high-copy bacterial plasmid. The temperature range of 56-58°C provided strong fluorescent signals and yielded no probe cross-reactivity. Therefore, the manufacturers' recommended thermo-cycling protocol with a 58°C annealing/extension step were carried out. Figure 3.1 shows experimental data from a representative ddPCR titration experiment demonstrating 100% probe specificity using linear plasmid DNA as PCR

template. All data analysis was performed using the accompanying platform software, QuantaSoft (Bio-Rad), with all reported values calculated using Poisson statistics.

Targeted Next-Generation DNA Sequencing

The proband's archival tissue derived genomic DNA (both tumor and surrounding normal) was subjected to targeted next-generation DNA sequencing using a custom 484 cancer gene panel. Targeted coding exon enrichment was carried out using Agilent's SureSelect technology and DNA sequencing was performed on an Illumina HiSeq 2000 platform. Resultant data was aligned to human genome 19 using BWA 0.6.1 (137) and variants were called using GATK 1.4 (138).

Results

To confirm the presence of the *BRCA2*^{M2322I} (c.6966G>T) variant in the two affected family members, exon 13 of *BRCA2* from buccal cell derived gDNA was sequenced. Consistent with previous genetic testing, both individuals diagnosed with cancer harbored the VUS. In addition, a heterozygous single nucleotide polymorphism (SNP) located within exon 11 of *BRCA2*, rs543304, was identified for the proband and her mother. The rs543304 SNP is located in exon 11 approximately 8.7 kilobases upstream on gDNA from the VUS, as illustrated in Figure 3.2a. Sanger sequencing traces derived from buccal cell gDNA depicting the VUS and rs543304 SNP are shown in Figure 3.2b. Next, gDNA from FFPE tissue blocks for the proband and her mother was purified to perform LOH and sequencing analysis on macrodissected tumor and adjacent normal breast tissue. Using Sanger sequencing for both the proband and her mother the rs543304 SNP was found to be heterozygous (Figure 3.2c). However, as seen in the sequencing traces in Figure 3.2c, there was a high degree of variability in Sanger

sequencing results for the VUS locus. Both tumor samples appeared to have a 1:1 ratio of wild type to VUS alleles. In contrast, the proband's normal adjacent tissue, appeared to have a 2:1 wild type to VUS allelic ratio, while the mother's normal tissue seemingly contained a 1:2 wild type to VUS ratio. This type of variability in PCR sequencing is not uncommon with the use of FFPE derived DNA, particularly when using minute quantities of DNA. Therefore, in order to confirm that our tumor and normal samples were not inadvertently switched, since allelic ratios are more often changed in tumors, the DNA used for these analyses were used for candidate gene sequencing to identify somatic mutations. First, exons 9 and 20 of *PIK3CA* and all coding exons of *TP53* were sequenced, as these genes are frequently mutated in breast cancers (139, 140). Initial sequencing results revealed a heterozygous somatic mutation in exon 20 of *PIK3CA* (c.3140A>T; H1047L) in the mother's tumor gDNA, as shown in Figure 3.3a. The proband's DNA preparations exhibited no *PIK3CA* mutations and neither patient demonstrated a *TP53* mutation by Sanger sequencing. Since no somatic mutations were identified for the proband for *PIK3CA* or *TP53*, the tumor and adjacent normal genomic DNA was used for targeted next generation sequencing with a custom 484 cancer gene panel. Unique somatic alterations found only in the proband's tumor were identified and are shown in Figure 3.3b.

The identification of somatic mutations in the tumor samples strongly suggested that the identity of the samples is correct and they samples were not mistakenly switched. Therefore, the results with PCR and Sanger sequencing underscored the difficulty of determining allelic ratios and LOH using FFPE derived DNA. To more accurately measure the *BRCA2* allelic ratios, the relatively new technology of ddPCR was used to

perform LOH analyses. Briefly, ddPCR is carried out through the creation of nanoliter droplets acting as parallel single molecule PCR reactions (Figure 3.4a) (136). The identity of the DNA molecules within each droplet can then be resolved using conventional dual labeled fluorescent oligonucleotide probes. Following end-point PCR on a standard thermo-cycler, all droplets are then counted using a fluorescent droplet reader (Figure 3.4b). It is reasonable to hypothesize that ddPCR would be well suited for LOH analysis of FFPE derived DNA for a number of reasons. First, it requires low amounts of input DNA with very short PCR amplicon sizes (<100 bp). Second, ddPCR uses dual labeled probes that are capable of reliably discriminating between single base pair changes, such as SNPs and mutations. Third, ddPCR has the capacity to easily and accurately determine differences in copy number below 2-fold, which is the lower limit of reliable detection using conventional quantitative real time PCR (qPCR). Therefore, this approach was used to effectively count the number of *BRCA2* alleles present within the patients' DNA samples using allele specific probes. By comparing the number of *BRCA2* alleles present within our patients' samples it is possible to simultaneously assess LOH and quantify contaminating normal DNA, as illustrated in Figure 3.4b. Using conventional allele-specific fluorescent probes, differing by only one nucleotide at *BRCA2* c.6966G/T, the *BRCA2* allelic ratios were quantified within the normal and tumor FFPE gDNA for both individuals. As shown in Figure 3.5a, the allelic ratios (wild type:VUS) were determined to be approximately one in all tissue samples assayed. Absolute percentages of wild type to VUS alleles are shown in Figure 3.5b. Representative 2D droplet reading plots for each patient sample are shown in Figure 6. Overall, these data clearly show no evidence of LOH in either individual's tumor or

normal sample, and importantly underscore the inability of conventional PCR-Sanger sequencing to accurately determine allelic ratios using FFPE gDNA.

Table 3.1: Sanger sequencing primers

Locus	Forward/Reverse PCR Primers	Nested Sequencing Primer(s)
BRCA2 (rs543304)	5’-CTCCTTCATAAACTGGCCAG 5’-CTTCTGCAGAGGTACATCC	5’-GTGCCAGTAGTCATTTCAA
BRCA2 (c.6966)	5’-CTGTGAGTTATTTGGTGCATAG 5’-ACGGGAAGTGTTAACTTC	5’-GAGCATCTGTTACATTCACTG
PIK3CA (Exon 9)	5'-TGAAAATAAAGTCTTGCAATG 5'-ACCTGTGACTCCATAGAA	5'-GGGAAAAATATGACAAAGAAAGC
PIK3CA (Exon 20)	5'-GAAAGCCTCTCTAATTTTGT 5'-TCAGTTCAATGCATGCTGT	5'-TGTTACAAGGCTTATCTAGC

Table 3.2: ddPCR Primer and Probe Sequences

Primer/Probe		Sequence
BRCA2 exon 13	Forward	5'-CCTAGGCACAATAAAAGATCG
(c.6966)	Reverse	5'-GTCTTACCGAAAGGGTACAC
BRCA2 WT Probe		5'-[VIC]-catgatgCataaacaatc-[MGB]
BRCA2 VUS Probe		5'-[6-FAM]-catgatgAataaacaatc-[MGB]

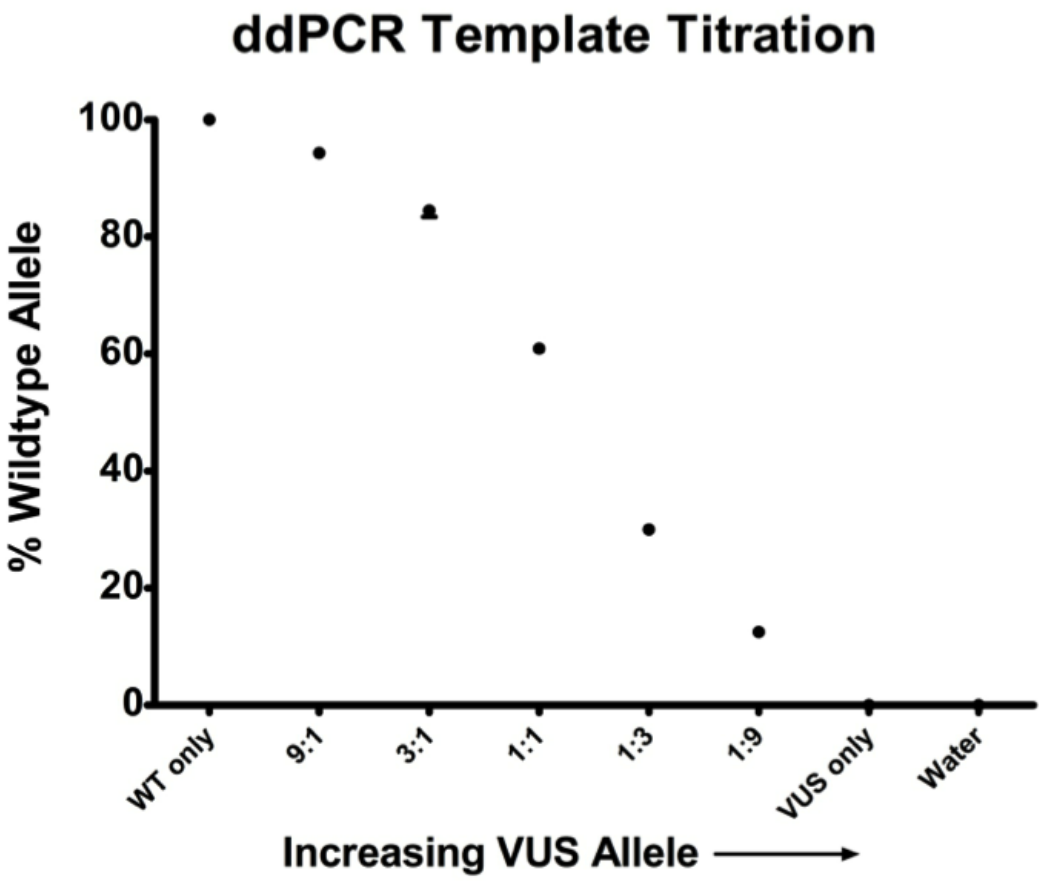

Figure 3.1: Titration plot showing 100% probe specificity for the optimized *BRCA2* ddPCR assay. Y-axis shows the % wildtype template as measured by ddPCR. *Hind* III linearized plasmids containing the respective *BRCA2* allele (wildtype or VUS) were used as PCR template. Droplets were gated using positive and negative controls.

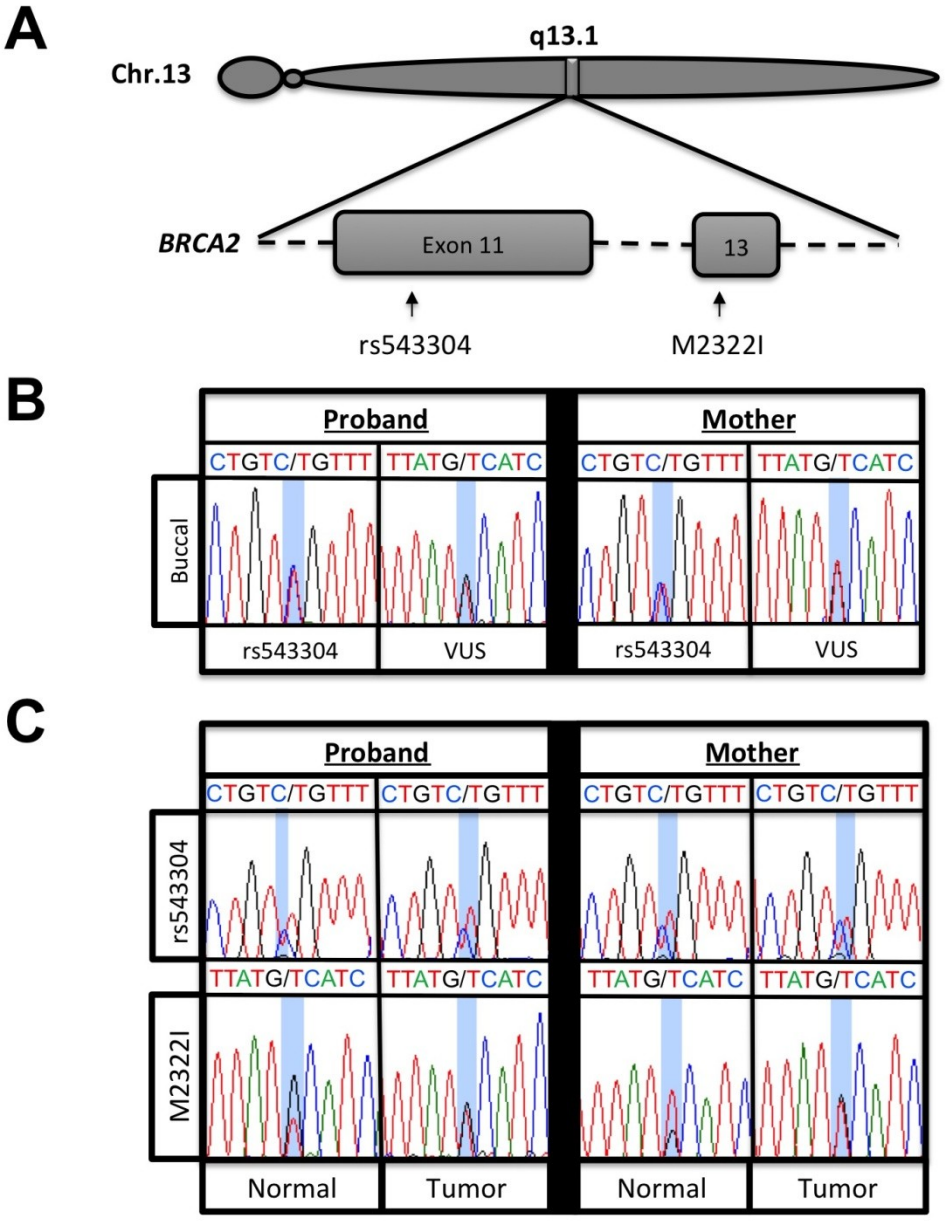

Figure 3.2: Sanger sequencing for *BRCA2* in proband and mother. A) Diagrammatic representation of *BRCA2* exons 11 and 13 showing the rs543304 SNP and c.6966G>T VUS, respectively. B) Sanger sequencing traces for both patient' buccal cell derived gDNA. C) *BRCA2* Sanger sequencing traces for both patients' FFPE derived gDNA.

A

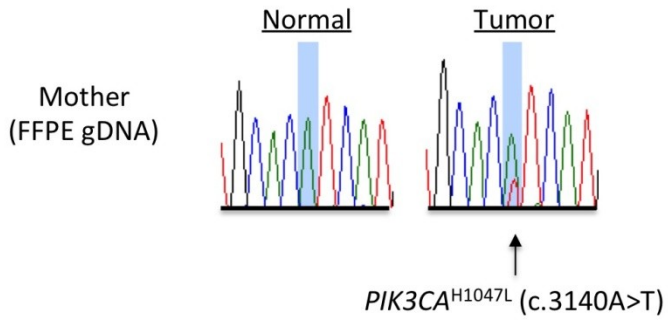

B

Gene Symbol	Accession # (mRNA)	Nucleotide (cDNA)	Amino Acid (Protein)	Mutation Type
ARHGAP26	NM_015071	c.2327C>T	S776L	Missense
BCL11A	NM_022893	c.2431G>A	V811M	Missense
CASC5	NM_144508	c.3775A>G	K1259E	Missense
CASC5	NM_144508	c.5341G>T	E1781X	Nonsense
CTNNB1	NM_001904	c.1544G>A	R515Q	Missense
EXT2	NM_001178083	c.406G>T	A136S	Missense
MED12	NM_005120	c.4673C>A	A1558D	Missense
NOTCH1	NM_017617	c.6209G>A	R2070Q	Missense
RET	NM_020630	c.1009G>A	E337K	Missense
SF3B1	NM_012433	c.2492G>A	R831Q	Missense
SH3GL1	NM_003025	c.550C>T	R184C	Missense
TET1	NM_030625	c.3769G>T	V1257F	Missense

Figure 3.3: Candidate gene sequencing results of patient samples. A) Sequencing traces showing somatic mutation in *PIK3CA* exon 20 (c.3140A>T; H1047L) in the mother's tumor. B) Table showing COSMIC filtered unique mutations found in the proband's tumor only.

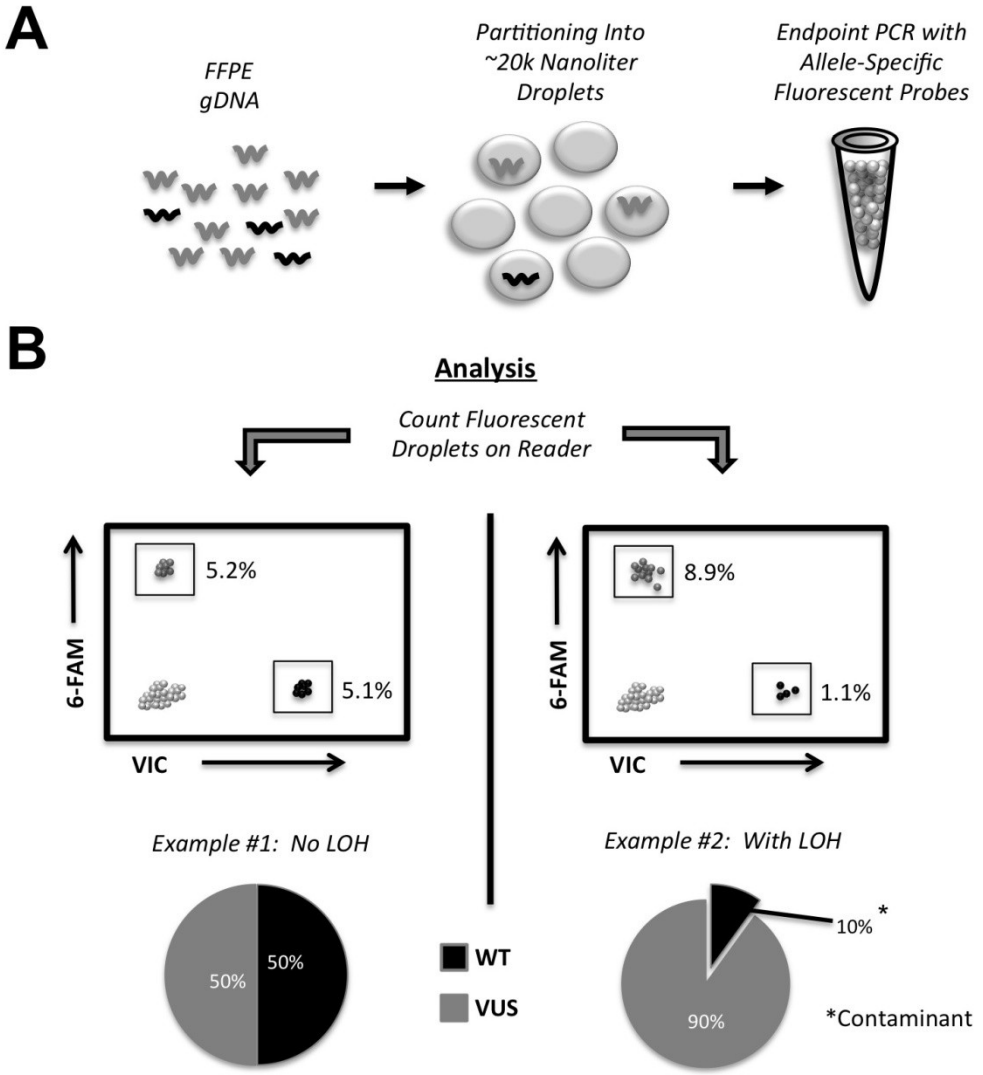

Figure 3.4: Schematic of ddPCR workflow for assessing LOH. A) The ddPCR reaction involves combining fragmented DNA to be studied with droplet oil and PCR reagents (PCR mastermix, primers and probes). The droplet generator machine partitions the required reagents and DNA fragments into approximately 2 x 10^4 individual droplets per well. Following droplet generation, end-point PCR is carried out on a standard thermo-cycler. B) After PCR amplification and generation of unquenched fluorophores, the droplets are read on a droplet reader. Example #1 illustrates the expected distribution of fluorescent droplets for no LOH, where 50% of the gated droplets are positive for the wild-type allele and 50% are positive for the VUS. Example #2 illustrates the approximate distribution of fluorescent droplets for LOH (with loss of the wild-type allele) with contaminating wild type from surrounding normal tissue.

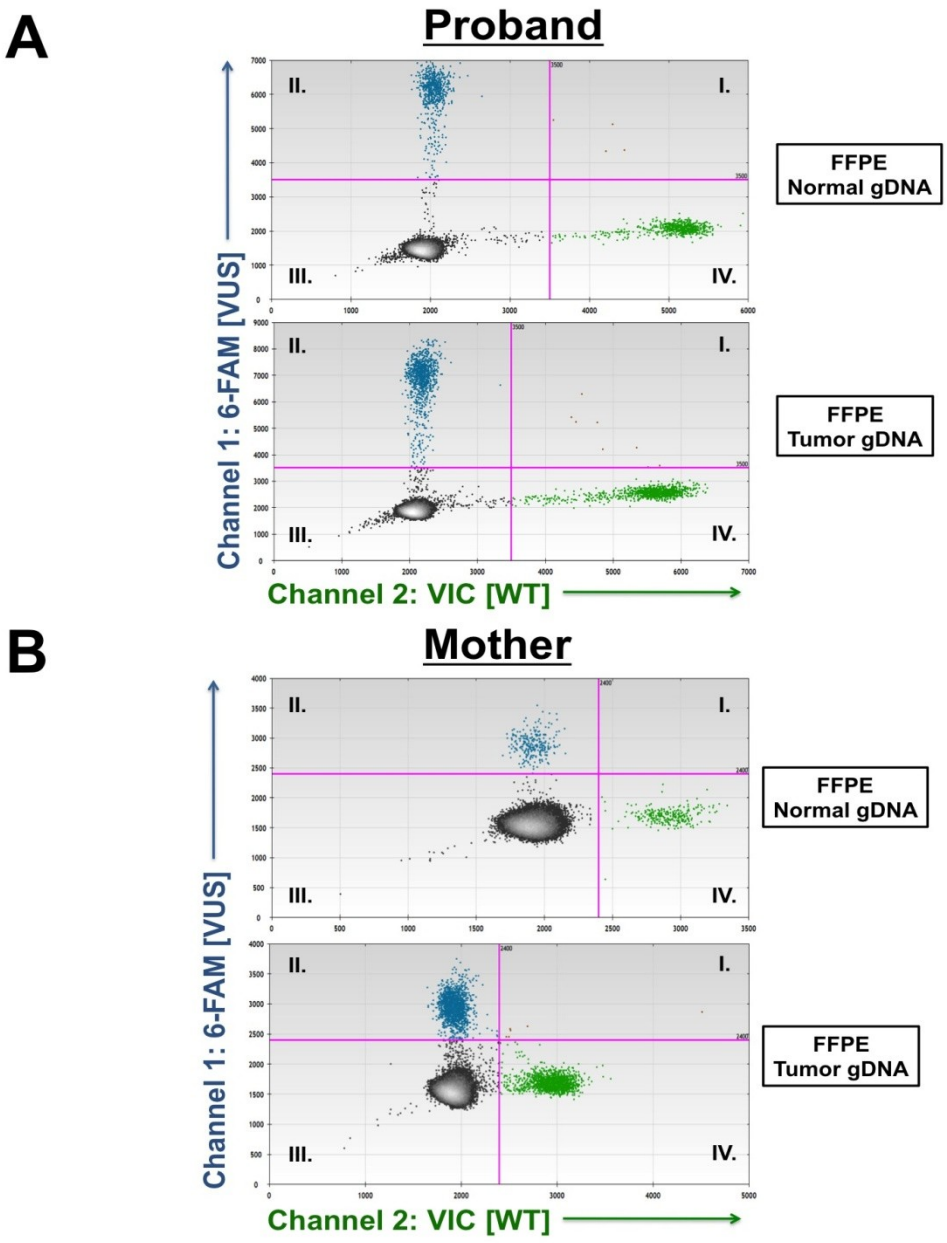

Figure 3.6: Representative droplet digital PCR results for the proband's (A) and the mother's (B) FFPE genomic DNA. Quadrant I = double positive gated droplets; Quadrant II = droplets gated positive for VUS allele; Quadrant III = negatively (empty) gated droplets; Quadrant IV = droplets gated positive for wildtype allele. Pink lines denote droplet gating thresholds.

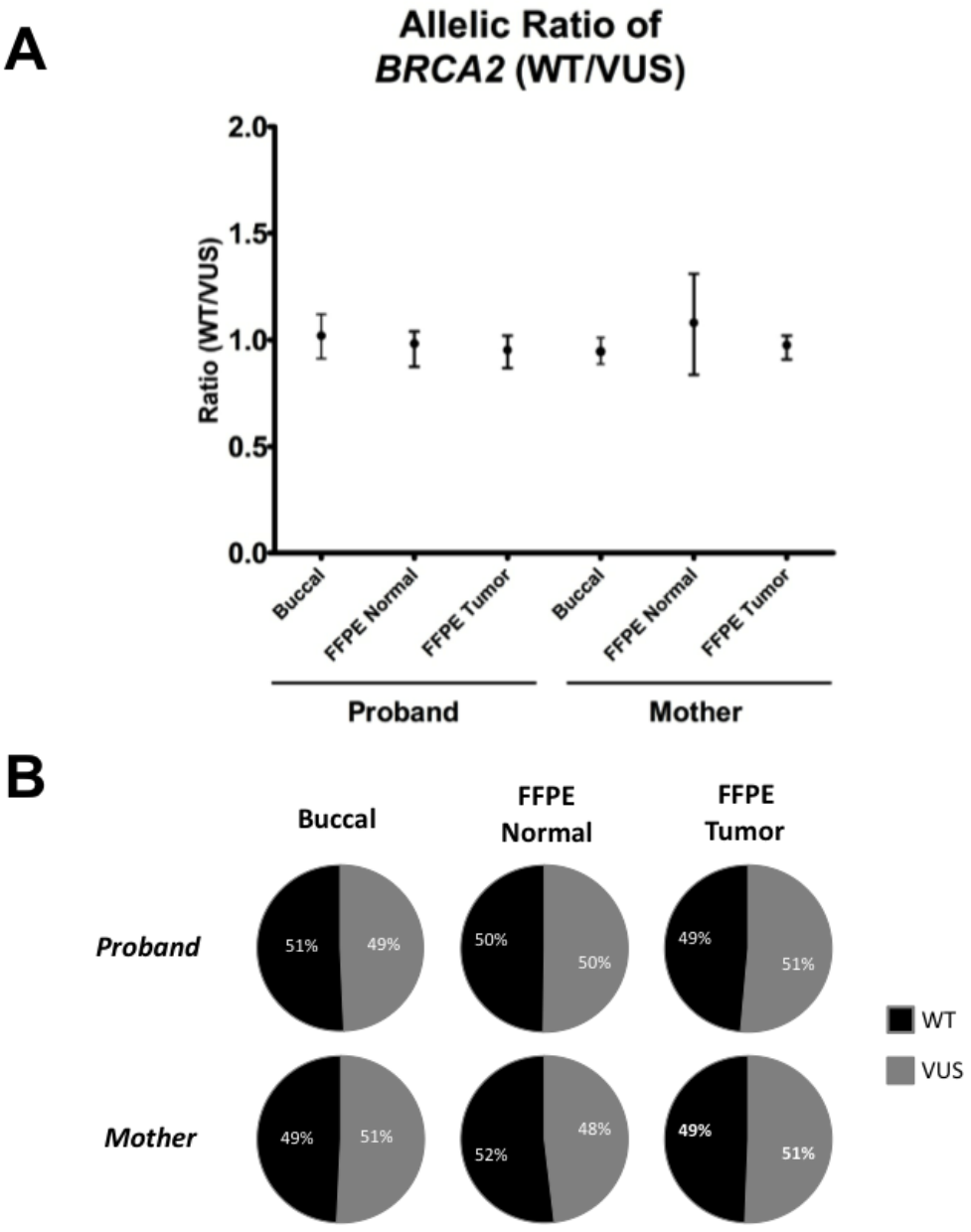

Figure 3.6: LOH analysis for the proband and her mother. A) Plot showing the allelic ratio (Wild type:VUS) measured for the buccal and FFPE DNA patient samples with standard error shown using Poisson statistics. B) Average percentage of fluorescent droplets corresponding to the VUS and wild type alleles for all patient samples. .

4 Discussion

BRCA VUS pose a formidable challenge to hereditary breast and ovarian cancer prevention. Approximately half of the nearly 4,000 cataloged *BRCA* alleles in the BIC are currently designated as VUS. To combat this ongoing problem many studies have been developed towards classifying VUS (103–105, 141). Arguably the most effective approaches utilize a number of clinically relevant features to calculate a likelihood score that a given VUS is deleterious. Often, however, the number of reported carriers for a given VUS is very small, sometimes consisting of only one individual. These small sample sizes coupled with the incomplete penetrance of *BRCA*-linked disease and the high incidence of sporadic breast cancer leads to insignificant statistical predictions. Therefore, investigators have turned to other modeling approaches, namely *in silico* analysis and direct functional testing.

Isogenic Cell Modeling of *BRCA1* Alleles

Isogenic cell modeling of *BRCA1* alleles, distinct from other *in vitro* functional tests, boasts several advantages that make it an attractive alternative to prior *BRCA1* modeling approaches. First, isogenic modeling in non-cancerous human breast epithelial cells permits investigators to evaluate BRCA1 function within the appropriate cellular context; non-cancerous human breast cells. Many of the prior studies have not done so, where they studied BRCA1 function in either human breast cancer cell lines or mouse embryonic stem cells. Secondly, isogenic cell modeling facilitates BRCA1 study at appropriate dosages via the control of the endogenous machinery. Prior studies have used exogenously expressed human *BRCA1* cDNA, and as a result studied BRCA1 function at artificially high levels. Thirdly, since isogenic modeling can be carried out in different genetically stable cell lines, it permits the interrogation of *BRCA1* function under genetically defined conditions, thereby potentially providing new insight into the effects of genetic modifiers. Lastly, this methodology also possesses the advantage of expandability. As a clearer understanding of BRCA1 function evolves, additional characterizing assays may be adapted for *in vitro* study.

Here we used isogenic modeling to evaluate functional differences between nine clinically important *BRCA1* alleles, including three deleterious, five VUS and one benign variant. Several conclusions can be made from experiments described herein. First, it seems that not all *BRCA1* deleterious mutations confer the same level of functional loss *in vitro*. That is, it appears that truncating *BRCA1* mutations lead to a higher level of sensitivity to ionizing radiation and genomic instability, as compared to other cancer causing *BRCA1* missense mutations. Whether these functional differences influence disease penetrance remains to be determined. Secondly, our data suggest isogenic cell

modeling may be useful for providing functional evidence for VUS classification efforts, where here we describe the functional effects of five VUS. Characterization of the C64R variant suggests this mutation is at least equally as deleterious as the C61G mutation, since cells harboring this mutation were sensitive to ionizing radiation and demonstrated increased genomic instability and centrosome amplification. Functional characterization of the D67Y mutation suggests it may be hypomorphic. As this mutation has previously been predicted to be benign, it may be that certain hypomorphs do not increase cancer risk in carriers. However, this also remains to be seen. Similarly, the cells harboring the S316G and Q356R only scored in one assay each, suggesting both may have hypomorphic properties. Despite the suppressed growth rate observed for cells harboring the L246V VUS, this variant did not demonstrate an appreciable difference from controls in the other assays, suggesting this variant may be benign. Nonetheless, further work is needed to determine if our *in vitro* model accurately reflects *in vivo* phenomena, and ultimately relative disease risk.

Like most models, the approach taken here does have some caveats. First, only one breast cell line, MCF-10A, was used to generate our *BRCA1* panel. It is possible that pre-existing genetic modifiers present within the MCF-10A genome influence the effects observed for the engineered mutations. To circumvent this problem, it would be necessary for future studies to employ other human non-tumorigenic breast cell lines, such as the hTERT immortalized breast epithelial cell line (hTERT-IMEC) we utilized in our previous isogenic studies with the *BRCA1*^{185delAG} alteration (62). Another potential shortcoming with the approach taken here resides in the employed gene targeting method, rAAV. rAAV-mediated gene-targeting is far from ideal, where it can be laborious, leaves

exogenous sequence following targeting (i.e. *loxP* scar DNA) and is susceptible to random integration of the targeting construct. Newer, alternative gene targeting methods, such as the CRISPR system, may overcome these problems (142). The very high targeting efficiency of the CRISPR system make it ideal for fast, selection free gene targeting. Finally, the number of deleterious and benign mutations engineered in this study is too small to make broader conclusions about the clinical applicability of isogenic modeling for *BRCA1* allele risk assessment. Further work is needed to translate our *in vitro BRCA1* haploinsufficiency observations towards clinical utility.

In accordance with previous work, and the work of others, we present further evidence for the hypothesis that mammary epithelial cells harboring a deleterious *BRCA1* allele are haploinsufficient for BRCA1. The results from our γ-irradiation experiments may have important implications for the current screening mammography paradigm in *BRCA* carriers. Consistent with previous studies showing that X-ray screening in *BRCA* carriers may increase cancer risk (143), the cells harboring a deleterious allele demonstrated increased radio-sensitivity. Presumably the increase in sensitivity is due to the cell's inability to repair DNA damage caused by the ionizing radiation. Therefore, MRI may be a safer alternative for screening within this cohort (144). In summary isogenic modeling of BRCA1 alleles is useful for study of disease causing alleles and alleles not clearly linked to cancer.

ddPCR Mediated LOH Analysis

LOH analysis, in combination with other methods, is useful in classifying uncertain *BRCA* variants. Although loss of the wild-type allele in tumor tissues provides

strong evidence for a deleterious germline mutation, it should be noted that absence of LOH cannot be used as a definitive criterion, since other mechanisms of inactivation of the wild-type allele exist. This would include epigenetic silencing as well as a *de novo* inactivating mutation within the wild-type allele. Nonetheless, given that loss of the second allele is an accepted common mechanism of carcinogenesis mediated by tumor suppressor genes in familial cancer syndromes, the studies described here have great potential for definitively assessing LOH and helping to ascribe a functional significance to germline VUS and deleterious mutations.

The arrival of commercially available digital PCR platforms has the potential to dramatically alter the speed and sensitivity of many molecular biology assays commonly used in the clinic. Others have shown that ddPCR can accurately determine both copy number changes and expression of critical oncogenes using patient samples (145, 146). This approach may prove to be a more objective and accurate measure for determining oncogene amplification and overexpression in cancer patients. Droplet digital PCR is especially useful for analysis of FFPE derived gDNA, since it relies on short DNA fragments and FFPE gDNA is generally highly fragmented. Moreover, since ddPCR queries individual DNA molecules, this approach should prove useful in several assays including determining the fractional abundance of somatic mutations within heterogeneous tumor tissue specimens, validation of somatic mutations identified using whole genome sequencing that are below the limit of detection by Sanger sequencing, and as demonstrated here, determining the allelic fraction of a given gene for LOH analysis. Although in principle, next generation sequencing using a targeted gene capture approach could also be used for LOH and copy number analysis, ddPCR offers

significant advantages including a much faster and cost efficient platform, need for less input DNA, superior sensitivity, no artifactual errors inherent with next generation sequencing, and no requirement for a bioinformatics pipeline for variant calling. To our knowledge, this is the first report demonstrating the utility of using ddPCR for accurately assessing allelic ratios via SNPs in FFPE tumor samples. This approach should greatly facilitate not only *BRCA* VUS LOH studies, but studies for other variants of genes implicated in hereditary cancer susceptibility.

References

1. Stratton MR, Campbell PJ, Futreal PA (2009) The Cancer Genome. *Nature* 458:719–24.
2. Foulkes WD (2008) Inherited susceptibility to common cancers. *N Engl J Med* 359:2143–53.
3. Stephens F, Gardner E, Woolf C (1958) A Recheck Of Kindred 107, Which Has Shown A High Frequency Of Breast Cancer. *Cancer* 11:967–972.
4. Fearon ER (1997) Human Cancer Syndromes: Clues to the Origin and Nature of Cancer. *Science* 278:1043–1050.
5. Hall J, Lee M, Newman B, Morrow J (1990) Linkage of early-onset familial breast cancer to chromosome 17q21. *Science* 250:1684–1689.
6. Knudson AG (1971) Mutation and cancer: statistical study of retinoblastoma. *Proc Natl Acad Sci U S A* 68:820–3.
7. Futreal P, Söderkvist P, Marks J (1992) Detection of Frequent Allelic Loss on Proximal Chromosome 17q in Sporadic Breast Carcinoma Using Microsatellite Length Polymorphisms. *Cancer Res* 52:2624–2627.
8. Smith S, Easton D, Evans D, Ponder B (1992) Allele losses in the region 17q12-21 in familial breast and ovarian cancer involve the wild-type chromosome. *Nat Genet* 2:128–131.
9. Miki Y et al. (1994) Strong Candidate for the Breast and Ovarian Cancer. *Science* 266.
10. Futreal P a et al. (1994) BRCA1 mutations in primary breast and ovarian carcinomas. *Science* 266:120–2.

11. Catteau A, Harris WH, Xu CF, Solomon E (1999) Methylation of the BRCA1 promoter region in sporadic breast and ovarian cancer: correlation with disease characteristics. *Oncogene* 18:1957–65.

12. Stratton MR et al. (1994) Familial male breast cancer is not linked to the BRCA1 locus on chromsome 17q. *Nat Genet* 7:103–107.

13. Wooster R, Neuhausen S, Mangion J, Quirk Y (1994) Localization of a Breast Cancer Susceptibility Gene, BRCA2, to Chromosome 13q12-13. *Science* 265:2088–2090.

14. Wooster R, Bignell G, Lancaster J, Swift S (1995) Identification of the breast cancer susceptibility gene BRCA2. *Nature* 378:789–792.

15. Collins N et al. (1995) Consistent loss of the wild type allele in breast cancers from a family linked to the BRCA2 gene on chromosome 13q12-13. *Oncogene* 10:1673–1675.

16. Özcelik H, Schmocker B, Nicola N Di (1997) Germline BRCA2 6174delT mutations in Ashkenazi Jewish pancreatic cancer patients. *Nat Genet* 16:17–18.

17. Edwards SM et al. (2003) Two percent of men with early-onset prostate cancer harbor germline mutations in the BRCA2 gene. *Am J Hum Genet* 72:1–12.

18. Howlett NG et al. (2002) Biallelic inactivation of BRCA2 in Fanconi anemia. *Science* 297:606–9.

19. Szabo C, Masiello A, Ryan JF, Brody LC (2000) The breast cancer information core: database design, structure, and scope. *Hum Mutat* 16:123–31.

20. Ruffner H, Verma IM (1997) BRCA1 is a cell cycle-regulated nuclear phosphoprotein. *Proc Natl Acad Sci U S A* 94:7138–43.

21. Wilson C a et al. (1997) Differential subcellular localization, expression and biological toxicity of BRCA1 and the splice variant BRCA1-delta11b. *Oncogene* 14:1–16.

22. ElShamy WM, Livingston DM (2004) Identification of BRCA1-IRIS, a BRCA1 locus product. *Nat Cell Biol* 6:954–67.

23. Merajver SD et al. (1995) Germline BRCA1 mutations and loss of the wild-type allele in tumors from families with early onset breast and ovarian cancer. *Clin Cancer Res* 1:539–44.

24. Castilla L, Couch F, Erdos M (1994) Mutations in the BRCA1 gene in families with early-onset breast and ovarian cancer. *Nat Genet* 8:387–391.

25. Friedman L, Szabo C (1995) Novel inherited mutations and variable expressivity of BRCA1 alleles, including the founder mutation 185delAG in Ashkenazi Jewish families. *Am J Hum Genet* 57:1284–1297.

26. Koonin E, Altschul S, Bork P (1996) BRCA1 protein products: functional motifs. *Nat Genet* 13:266–268.

27. Callebaut I, Mornon JP (1997) From BRCA1 to RAP1: a widespread BRCT module closely associated with DNA repair. *FEBS Lett* 400:25–30.

28. Yu X, Chini CCS, He M, Mer G, Chen J (2003) The BRCT domain is a phospho-protein binding domain. *Science* 302:639–42.

29. Manke I a, Lowery DM, Nguyen A, Yaffe MB (2003) BRCT repeats as phosphopeptide-binding modules involved in protein targeting. *Science* 302:636–9.

30. Leung CCY, Glover JNM (2011) BRCT domains: Easy as one, two, three. *Cell Cycle* 10:2461–2470.

31. Bork P, Hofmann K, Bucher P (1997) A superfamily responsive of conserved domains in DNA damage-responsive cell cycle checkpoint proteins. *FASEB J* 11:68–76.

32. Freemont PS, Hanson IM, Trowsdale J (1991) A Novel Cysteine-Rich Sequence Motif. *Cell* 64:483–484.

33. Ruffner H, Joazeiro C a, Hemmati D, Hunter T, Verma IM (2001) Cancer-predisposing mutations within the RING domain of BRCA1: loss of ubiquitin protein ligase activity and protection from radiation hypersensitivity. *Proc Natl Acad Sci U S A* 98:5134–9.

34. Hashizume R et al. (2001) The RING heterodimer BRCA1-BARD1 is a ubiquitin ligase inactivated by a breast cancer-derived mutation. *J Biol Chem* 276:14537–40.

35. Silver DP, Livingston DM (2012) Mechanisms of BRCA1 tumor suppression. *Cancer Discov* 2:679–84.

36. Wu L, Wang Z, Tsan J, Spillman M (1996) Identification of a RING protein that can interact in vivo with the BRCA1 gene product. *Nat Genet* 14.

37. Brzovic PS, Meza J, King MC, Klevit RE (1998) The cancer-predisposing mutation C61G disrupts homodimer formation in the NH2-terminal BRCA1 RING finger domain. *J Biol Chem* 273:7795–9.

38. Joukov V, Chen J, Fox E a, Green JB, Livingston DM (2001) Functional communication between endogenous BRCA1 and its partner, BARD1, during Xenopus laevis development. *Proc Natl Acad Sci U S A* 98:12078–83.

39. Drost R et al. (2011) BRCA1 RING function is essential for tumor suppression but dispensable for therapy resistance. *Cancer Cell* 20:797–809.

40. Shakya R et al. (2011) BRCA1 tumor suppression depends on BRCT phosphoprotein binding, but not its E3 ligase activity. *Science (80-)* 334:525–8.

41. Zhu Q et al. (2011) BRCA1 tumour suppression occurs via heterochromatin-mediated silencing. *Nature* 477:179–84.

42. Matsuzawa A et al. (2013) The BRCA1/BARD1-Interacting Protein OLA1 Functions in Centrosome Regulation. *Mol Cell* 53:101–114.

43. Tavtigian S, Simard J, Rommens J (1996) The complete BRCA2 gene and mutations in chromosome 13q-linked kindreds. *Nat Genet* 12:333–337.

44. Chen PL et al. (1998) The BRC repeats in BRCA2 are critical for RAD51 binding and resistance to methyl methanesulfonate treatment. *Proc Natl Acad Sci U S A* 95:5287–92.

45. Pellegrini L et al. (2002) Insights into DNA recombination from the structure of a RAD51-BRCA2 complex. *Nature* 420:287–93.

46. Jeyasekharan AD et al. (2013) A cancer-associated BRCA2 mutation reveals masked nuclear export signals controlling localization. *Nat Struct Mol Biol* 20:1191–8.

47. Chapman M, Verma I (1996) Transcriptional activation by BRCA1. *Nature* 382:678–679.

48. Mullan PB, Quinn JE, Harkin DP (2006) The role of BRCA1 in transcriptional regulation and cell cycle control. *Oncogene* 25:5854–63.

49. Moynahan ME, Chiu JW, Koller BH, Jasin M (1999) Brca1 controls homology-directed DNA repair. *Mol Cell* 4:511–8.

50. Huen MSY, Sy SMH, Chen J (2010) BRCA1 and its toolbox for the maintenance of genome integrity. *Nat Rev Mol Cell Biol cell Biol* 11:138–48.

51. Hakem R, Pompa J de la, Elia A, Potter J, Mak T (1997) Partial rescue of brca1 early embryonic lethality by p53 or p21 null mutation. *Nat Genet* 16:298–302.

52. Somasundaram K, Zhang H, Zeng Y (1997) Arrest of the cell cycle by the tumour-suppressor BRCA1 requires the CDK-inhibitor p21. *Nature*:187–190.

53. Xu X et al. (1999) Centrosome amplification and a defective G2-M cell cycle checkpoint induce genetic instability in BRCA1 exon 11 isoform-deficient cells. *Mol Cell* 3:389–95.

54. Hsu LC, White RL (1998) BRCA1 is associated with the centrosome during mitosis. *Proc Natl Acad Sci U S A* 95:12983–8.

55. Starita LM et al. (2004) BRCA1-Dependent Ubiquitination of γ-Tubulin Regulates Centrosome Number. *Mol Cell Biol* 24:8457–8466.

56. Parvin JD, Sankaran S (2006) The BRCA1 E3 ubiquitin ligase controls centrosome dynamics. *Cell Cycle* 5:1946–50.

57. Chang S et al. (2011) Tumor suppressor BRCA1 epigenetically controls oncogenic microRNA-155. *Nat Med* 17:1275–1282.

58. Liu CY, Flesken-Nikitin A, Li S, Zeng Y, Lee WH (1996) Inactivation of the mouse Brca1 gene leads to failure in the morphogenesis of the egg cylinder in early postimplantation development. *Genes Dev* 10:1835–1843.

59. Hakem R et al. (1996) The tumor suppressor gene Brca1 is required for embryonic cellular proliferation in the mouse. *Cell* 85:1009–23.

60. Gowen L, Johnson B, Latour A (1996) Brca1 deficiency results in early embryonic lethality characterized by neuroepithelial abnormalities. *Nat Genet* 12:191–194.

61. Martins FC et al. (2012) Evolutionary pathways in BRCA1-associated breast tumors. *Cancer Discov* 2:503–11.

62. Konishi H et al. (2011) Mutation of a single allele of the cancer susceptibility gene BRCA1 leads to genomic instability in human breast epithelial cells. *Proc Natl Acad Sci U S A* 108:17773–8.

63. Buchholz TA et al. (2002) Evidence of haplotype insufficiency in human cells containing a germline mutation in BRCA1 or BRCA2. *Int J Cancer* 561:557–561.

64. Bellacosa A et al. (2010) Altered gene expression in morphologically normal epithelial cells from heterozygous carriers of BRCA1 or BRCA2 mutations. *Cancer Prev Res* 3:48–61.

65. Boyd M, Harris F, McFarlane R (1995) A human BRCA1 gene knockout. *Nature* 375:541–542.

66. Domchek SM et al. (2013) Biallelic deleterious BRCA1 mutations in a woman with early-onset ovarian cancer. *Cancer Discov* 3:399–405.

67. Kuschel B, Gayther S a, Easton DF, Ponder B a, Pharoah PD (2001) Apparent human BRCA1 knockout caused by mispriming during polymerase chain reaction: implications for genetic testing. *Genes Chromosomes Cancer* 31:96–8.

68. Liede a et al. (2000) Evidence of a founder BRCA1 mutation in Scotland. *Br J Cancer* 82:705–11.

69. Scully R et al. (1997) Association of BRCA1 with Rad51 in mitotic and meiotic cells. *Cell* 88:265–75.

70. Scully R et al. (1999) Genetic analysis of BRCA1 function in a defined tumor cell line. *Mol Cell* 4:1093–9.

71. Tomlinson GE et al. (1998) Characterization of a breast cancer cell line derived from a germ-line BRCA1 mutation carrier. *Cancer Res* 58:3237–42.

72. Bunting SF et al. (2012) BRCA1 functions independently of homologous recombination in DNA interstrand crosslink repair. *Mol Cell* 46:125–35.

73. Roy R, Chun J, Powell SN (2012) BRCA1 and BRCA2 : different roles in a common pathway of genome protection. *Nat Rev Cancer* 12:68–78.

74. Parvin JD (2009) The BRCA1-Dependent Ubiquitin Ligase, ɣ-Tubulin, and Centrosomes. *Environ Mol Mutagen*:649–653.

75. Shyam SK et al. (1997) Embryonic lethality and radiation hypersensitivity mediated by Rad51 in mice lacking Brca2. *Nature* 386:804–810.

76. Moynahan ME, Pierce AJ, Jasin M (2001) BRCA2 is required for homology-directed repair of chromosomal breaks. *Mol Cell* 7:263–72.

77. Branzei D, Foiani M (2010) Maintaining genome stability at the replication fork. *Nat Rev Mol Cell Biol* 11:208–19.

78. Moynahan ME, Jasin M (2010) Mitotic homologous recombination maintains genomic stability and suppresses tumorigenesis. *Nat Rev Mol Cell Biol* 11:196–207.

79. Consortium BCL (1997) Pathology of familial breast cancer: differences between breast cancers in carriers of BRCA1 or BRCA2 mutations and sporadic cases. *Lancet* 349:1505–1510.

80. Brown D, Cole B, Arrick B (1999) RESPONSE: more about: multifactorial analysis of differences between sporadic breast cancers and cancers involving BRCA1 and BRCA2 mutations. *J Natl Cancer Inst* 91:1138–1145.

81. Mavaddat N et al. (2012) Pathology of breast and ovarian cancers among BRCA1 and BRCA2 mutation carriers: results from the Consortium of Investigators of Modifiers of BRCA1/2 (CIMBA). *Cancer Epidemiol Biomarkers Prev* 21:134–47.

82. Lakhani SR, Reis-Filho JS, Fulford L (2005) Prediction of BRCA1 Status in Patients with Breast Cancer Using Estrogen Receptor and Basal Phenotype. *Clin Cancer Res* 11:5175–5180.

83. Holstege H et al. (2009) High incidence of protein-truncating TP53 mutations in BRCA1-related breast cancer. *Cancer Res* 69:3625–33.

84. Manié E et al. (2009) High frequency of TP53 mutation in BRCA1 and sporadic basal-like carcinomas but not in BRCA1 luminal breast tumors. *Cancer Res* 69:663–71.

85. Greenblatt M, Chappuis P, Bond J (2001) TP53 Mutations in Breast Cancer Associated with BRCA1 or BRCA2 Germ-line Mutations. *Cancer Res*:4092–4097.

86. Crook T, Crossland S, Crompton M (1997) p53 mutations in BRCA1-associated familial breast cancer. *Lancet* 350:638–639.

87. Ford D et al. (1998) Genetic Heterogeneity and Penetrance Analysis of the BRCA1 and BRCA2 Genes in Breast Cancer Families. *Am J Hum Genet* 1:676–689.

88. Easton DF, Ford D, Bishop DT, Linkage C (1995) Breast and Ovarian Cancer Incidence in BRCA1 Mutation Carriers. *Am J Hum Genet*:265–271.

89. Easton D, Steele L, Fields P (1997) Cancer Risks in Two Large Breast Cancer Families Linked to BRCA2 on Chromosome 13q12-13. *Am J Hum Genet*:120–128.

90. Narod SA, Foulkes WD (2004) BRCA1 and BRCA2: 1994 and beyond. *Nat Rev Cancer* 4:665–76.

91. Antoniou a et al. (2003) Average risks of breast and ovarian cancer associated with BRCA1 or BRCA2 mutations detected in case Series unselected for family history: a combined analysis of 22 studies. *Am J Hum Genet* 72:1117–30.

92. Couch FJ, Nathanson KL, Offit K (2014) Two decades after BRCA: setting paradigms in personalized cancer care and prevention. *Science* 343:1466–70.

93. Rebbeck TR et al. (1999) Breast cancer risk after bilateral prophylactic oophorectomy in BRCA1 mutation carriers. *J Natl Cancer Inst* 91:1475–9.

94. Rebbeck TR et al. (2004) Bilateral prophylactic mastectomy reduces breast cancer risk in BRCA1 and BRCA2 mutation carriers: the PROSE Study Group. *J Clin Oncol* 22:1055–62.

95. Bryant HE et al. (2005) Specific killing of BRCA2-deficient tumours with inhibitors of poly(ADP-ribose) polymerase. *Nature* 434:913–7.

96. Farmer H et al. (2005) Targeting the DNA repair defect in BRCA mutant cells as a therapeutic strategy. *Nature* 434:917–21.

97. Curtin N (2014) PARP inhibitors for anticancer therapy. *Biochem Soc Trans* 42:82–8.

98. Maxwell KN, Domchek SM (2012) Cancer treatment according to BRCA1 and BRCA2 mutations. *Nat Rev Clin Oncol* 9:520–8.

99. O'Shaughnessy J et al. (2011) Iniparib plus chemotherapy in metastatic triple-negative breast cancer. *N Engl J Med* 364:205–214.

100. Norquist B et al. (2011) Secondary somatic mutations restoring BRCA1/2 predict chemotherapy resistance in hereditary ovarian carcinomas. *J Clin Oncol* 29:3008–15.

101. Kaye SB et al. (2012) Phase II, open-label, randomized, multicenter study comparing the efficacy and safety of olaparib, a poly (ADP-ribose) polymerase inhibitor, and pegylated liposomal doxorubicin in patients with BRCA1 or BRCA2 mutations and recurrent ovarian cancer. *J Clin Oncol* 30:372–9.

102. Fong P, Boss D, Yap T, Tutt A (2009) Inhibition of Poly(ADP-Ribose) Polymerase in Tumors from BRCA Mutation Carriers. *N Engl J Med* 361:123–134.

103. Lindor NM et al. (2012) A review of a multifactorial probability-based model for classification of BRCA1 and BRCA2 variants of uncertain significance (VUS). *Hum Mutat* 33:8–21.

104. Millot G a et al. (2012) A guide for functional analysis of BRCA1 variants of uncertain significance. *Hum Mutat*:1–12.

105. Spearman AD et al. (2008) Clinically applicable models to characterize BRCA1 and BRCA2 variants of uncertain significance. *J Clin Oncol* 26:5393–400.

106. Carvalho MA, Couch FJ, Monteiro AN (2007) Functional assays for BRCA1 and BRCA2. *Int J Biochem Cell Biol* 39:298–310.

107. Ransburgh DJR, Chiba N, Ishioka C, Toland AE, Parvin JD (2010) Identification of breast tumor mutations in BRCA1 that abolish its function in homologous DNA recombination. *Cancer Res* 70:988–95.

108. Kais Z, Chiba N, Ishioka C, Parvin JD (2012) Functional differences among BRCA1 missense mutations in the control of centrosome duplication. *Oncogene* 31:799–804.

109. Chang S, Biswas K, Martin B (2009) Expression of human BRCA1 variants in mouse ES cels allows functional analysis of BRCA1 mutations. *J Clin Invest* 119.

110. Kuznetsov SG, Liu P, Sharan SK (2008) Mouse embryonic stem cell-based functional assay to evaluate mutations in BRCA2. *Nat Med* 14:875–81.

111. Bouwman P et al. (2013) A high-throughput functional complementation assay for classification of BRCA1 missense variants. *Cancer Discov* 3:1142–55.

112. DiRenzo J et al. (2002) Growth Factor Requirements and Basal Phenotype of an Immortalized Mammary Epithelial Cell Line. *Cancer Res*:89–98.

113. Soule H, Maloney T, Wolman S (1990) Isolation and Characterization of a Spontaneously Immortalized Human Breast Epithelial Cell Line, MCF-10. *Cancer Res*:6075–6086.

114. Santarosa M, Ashworth A (2004) Haploinsufficiency for tumour suppressor genes: when you don't need to go all the way. *Biochim Biophys Acta* 1654:105–22.

115. Savage KI et al. (2014) Brca1 Deficiency Exacerbates Estrogen Induced Dna Damage and Genomic Instability. *Cancer Res*, in press.

116. Skehan P, Storeng R (1990) New Colorimetric Cytotoxicity Assay for Anticancer-Drug Screening. *J Natl Cancer Inst*:1107–1112.

117. Gustin JP et al. (2009) Knockin of mutant PIK3CA activates multiple oncogenic pathways. *Proc Natl Acad Sci U S A* 106:2835–40.

118. Wang GM et al. (2013) Single Copies of Mutant KRAS and Mutant PIK3CA Cooperate in Immortalized Human Epithelial Cells to Induce Tumor Formation. *Cancer Res* 73.

119. Topaloglu O, Hurley PJ, Yildirim O, Civin CI, Bunz F (2005) Improved methods for the generation of human gene knockout and knockin cell lines. *Nucleic Acids Res* 33:e158.

120. Ho SN, Hunt HD, Horton RM, Pullen JK, Pease LR (1989) Site-directed mutagenesis by overlap extension using the polymerase chain reaction. *Gene* 77:51–9.

121. Konishi H et al. (2007) A PCR-based high-throughput screen with multiround sample pooling: application to somatic cell gene targeting. *Nat Protoc* 2:2865–74.

122. Ransburgh DJR, Chiba N, Ishioka C, Toland AE, Parvin JD (2010) Identification of breast tumor mutations in BRCA1 that abolish its function in homologous DNA recombination. *Cancer Res* 70:988–95.

123. Easton DF et al. (2007) A systematic genetic assessment of 1,433 sequence variants of unknown clinical significance in the BRCA1 and BRCA2 breast cancer-predisposition genes. *Am J Hum Genet* 81:873–83.

124. Atipairin A, Ratanaphan A (2011) In Vitro Enhanced Sensitivity to Cisplatin in D67Y BRCA1 RING Domain Protein. *Breast Cancer* 5:201–8.

125. Zhong Q (1999) Association of BRCA1 with the hRad50-hMre11-p95 Complex and the DNA Damage Response. *Science* 285:747–750.

126. Ouchi T, Monteiro A, August A, Aaronson SA, Hanafusa H (1998) BRCA1 regulates p53-dependent gene expression. *Proc Natl Acad Sci U S A* 95:2302–2306.

127. Aprelikova ON et al. (1999) BRCA1-associated growth arrest is RB-dependent. *Proc Natl Acad Sci U S A* 96:11866–71.

128. Zhang H et al. (1998) BRCA1 physically associates with p53 and stimulates its transcriptional activity. *Oncogene* 16:1713–21.

129. Wang Q, Zhang H, Kajino K, Greene MI (1998) BRCA1 binds c-Myc and inhibits its transcriptional and transforming activity in cells. *Oncogene* 17:1939–48.

130. Vega A et al. (2001) The R71G BRCA1 is a founder Spanish mutation and leads to aberrant splicing of the transcript. *Hum Mutat* 17:520–1.

131. Lengauer C, Kinzler KW, Vogelstein B (1998) Genetic instabilities in human cancers. *Nature* 396:643–9.

132. Chenevix-Trench G et al. (2006) Genetic and histopathologic evaluation of BRCA1 and BRCA2 DNA sequence variants of unknown clinical significance. *Cancer Res* 66:2019–27.

133. Osorio A et al. (2002) Loss of heterozygosity analysis at the BRCA loci in tumor samples from patients with familial breast cancer. *Int J Cancer* 99:305–9.

134. Osorio A et al. (2007) Classification of missense variants of unknown significance in BRCA1 based on clinical and tumor information. *Hum Mutat* 28:477–485.

135. Karnan S et al. (2010) Controversial BRCA1 allelotypes in commonly used breast cancer cell lines. *Breast Cancer Res Treat* 119:249–51.

136. Hindson B et al. (2011) High-throughput droplet digital PCR system for absolute quantitation of DNA copy number. *Anal Chem* 83:8604–8610.

137. Li H, Durbin R (2009) Fast and accurate short read alignment with Burrows-Wheeler transform. *Bioinformatics* 25:1754–60.

138. McKenna A et al. (2010) The Genome Analysis Toolkit: a MapReduce framework for analyzing next-generation DNA sequencing data. *Genome Res* 20:1297–303.

139. Bachman K et al. (2004) The PIK3CA Gene is Mutated with High Frequency in Human Breast Cancers. *Cancer Biol Ther* 3:772–775.

140. Wood LD et al. (2007) The genomic landscapes of human breast and colorectal cancers. *Science* 318:1108–13.

141. Spurdle AB et al. (2012) ENIGMA--evidence-based network for the interpretation of germline mutant alleles: an international initiative to evaluate risk and clinical significance associated with sequence variation in BRCA1 and BRCA2 genes. *Hum Mutat* 33:2–7.

142. Mali P, Esvelt KM, Church GM (2013) Cas9 as a versatile tool for engineering biology. *Nat Methods* 10:957–63.

143. Gronwald J et al. (2008) Early radiation exposures and BRCA1-associated breast cancer in young women from Poland. *Breast Cancer Res Treat* 112:581–4.

144. Warner E et al. (2011) Prospective study of breast cancer incidence in women with a BRCA1 or BRCA2 mutation under surveillance with and without magnetic resonance imaging. *J Clin Oncol* 29:1664–9.

145. Belgrader P et al. (2013) Droplet Digital PCR Measurement of HER2 Copy Number Alteration in Formalin-Fixed Paraffin-Embedded Breast Carcinoma Tissue. *Clin Chem* 000:1–4.

146. Heredia NJ et al. (2013) Droplet Digital™ PCR quantitation of HER2 expression in FFPE breast cancer samples. *Methods* 59:S20–3.

Curriculum Vitae

Rory L. Cochran

1650 Orleans Street, CRB1 Rm. 128, Baltimore MD 21231
951.265.0869 | cochran.rory@gmail.com

Education

Ph.D. in Cellular & Molecular Medicine 2014
The Johns Hopkins University School of Medicine, Baltimore, MD
Thesis Advisor: Ben Ho Park, MD., Ph.D.
Thesis Dissertation: "Novel Approaches to Studying *BRCA* Variants of Unknown Clinical Significance"

B.S. in General Biology 2007
University of California San Diego, La Jolla, CA

Research Experience

The Johns Hopkins University School of Medicine 2009 – 2014
Ph.D. Graduate Student Baltimore, MD

Utilized modern viral-mediated gene targeting techniques to establish an *in vitro* model for studying different clinically reported *BRCA1* alleles. Also, developed a facile approach for assessing *BRCA2* loss-of-heterozygosity in archival tissue specimens using droplet digital PCR. Lastly, mentored and trained undergraduate, graduate and medical fellow laboratory trainees.

University of California San Diego 2008 – 2009
Research Associate II, Palmer Taylor Laboratory La Jolla, CA

Carried out recombinant protein mutagenesis studies on human acetylcholinesterase (hAChE) towards two objectives: i) develop a hAChE-based catalytic bio-scavenger for improving organophosphate toxicity treatment, and ii) study structural influences of surface residues on hAChE substrate catalysis.

University of California San Diego 2007 – 2009
Lab Manager, ScienceBridge Laboratories La Jolla, CA

Managed the overall laboratory operations of the UCSD ScienceBridge lab and off campus tech-sites. Developed a web-based quality control/materials tracking system, developed new experimental activities, managed quality control experiments, created an effective lab training curriculum for undergraduates, monitored experimental materials production, and supervised staff and volunteers.

Allele Biotechnology & Pharmaceuticals 2007 – 2008
Research Associate I San Diego, CA

Managed and processed the weekly retail orders for laboratory research products. Also, carried out most of the research and develop experiments for establishing new products.

University of California San Diego 2006 – 2007
Lab Assistant, ScienceBridge Laboratory La Jolla, CA

Carried out routine experiments to prepare materials for experimental activities, aided in creating new activities and determined optimal experimental conditions for established activities. Also, performed lab purchasing, wrote basic lab protocols, and trained and supervised undergraduate lab volunteers.

Academic Honors

University of California, San Diego
Provost's Honors:
- Winter 2006
- Spring 2006
- Winter 2007

Awards & Grants

National Cancer Institute 2012-2014
Ruth L. Kirschstein National Research Service Award (F31)
Title: "A Novel Model System for Risk Assessment of *BRCA* Carriers."

US Grants: University of California, San Diego 2007
Undergraduate Scholastic Research Grant ($250)

Publications

Blair, B.G., Wu, X., Zahari, M.S., Mohseni, M., Cidado, J., Wong, H.Y., Beaver, J.A., **Cochran, R.L.**, Zabransky, D.J., Croessmann, S., Chu, D., Toro, P.V., Cravero, K., Pandey, A. and Park, B.H. (2014). "A phosphoproteomic screen demonstrates differential dependence on HER3 for MAP kinase pathway activation by distinct *PIK3CA* mutations." *Submitted*

Mohseni, M., Cidado, J., Cimino-Mathews, A., Abukhdeir, A., Garay, J.P., Wang, G.W., Wong, H.Y., Croessmann, S., Beaver, J.A., **Cochran, R.L.**, Blair, B.G., Zabransky, D.J., Rosen, D.M., Argani, P., Hurley, P.J., Lauring, J. and Park, B.H. (2014). "*MACROD2* overexpression mediates estrogen independent growth and tamoxifen resistance in breast cancers." *Submitted*

Cidado, J., Rosen, D.R., Cimino-Mathews, A., Garay, J.P., Fessler, A.G., Rasheed, Z.A., Hicks, J., **Cochran, R.L.**, Wong, H.Y., Croessmann, S., Blair, B.G., Zabransky, D.J., Mohseni, M., Beaver, J.A., Chu, D., Cravero, K., De Marzo, A.M., Argani, P., Hurley, P.J., Lauring, J. and Park, B.H. (2014). "Gene disruption of Ki-67 alters properties associated with cancer stem cells." *Submitted*

Le, A., Stine, Z.E., Nguyen, C., Afzal, J., Sun, P., Hamaker, M., Siegel, N.M., Gouw, A.M., Kang, B., Yu, S., **Cochran, R.L.**, Sailor, K.A., Song, H. and Dang, C.V. (2014). "Tumorigenicity of hypoxic respiring cancer cells revealed by a hypoxia-cell cycle dual reporter." *PNAS,* in press.

*Forde, P.M., ***Cochran, R.L.**, Boikos, S.A., Zabransky, D.J., Beaver, J.A., Meyer, C.F., Thornton, K.A., Montgomery, E.A., Lidor, A.O., Donehower, R.C. & Park, B.H. (2014). "Familial Gastrointestinal Stromal Tumor with Loss-of-Heterozygosity and Amplification of Mutant *KIT*." *Journal of Clinical Oncology,* in press.

(*these authors contributed equally to this work)

***Cochran, R.L.**, *Cravero, K., Chu, D., Erlanger, B., Valda Toro, P., Beaver, J.A., Zabransky, D.J., Wong, H.Y., Cidado, J., Croessmann, S., Parsons, H., Kim, M., Wheelan, S.J., Argani, P. & Park, B.H. (2014). "Analysis of BRCA2 loss-of-heterozygosity in tumor tissue using droplet digital PCR." *Human Pathology*, 45(7): 1546-50.

(*these authors contributed equally to this work)

Beaver, J.A., Jelovac, D., Balukrishna, S., **Cochran, R.L.**, Croessmann, S., Zabransky, D.J., Wong, H.Y., Valda Toro, P., Cidado, J., Blair, B.G., Chu, D., Burns, T., Higgins, M.J., Stearns, V., Jacobs, L., Habibi, M., Lange, J., Hurley, P.J., Lauring, J., VanDenBerg, D., Kessler, J., Jeter, S., Samuels, M.L., Maar, D., Cope, L., Cimino-Mathews, A., Argani, P., Wolff, A.C. & Park, B.H. (2014). "Detection of Cancer DNA in Plasma of Early Stage Breast Cancer Patients." *Clinical Cancer Research,* 20(10): 2643-50.

Wang, G. M., Wong, H. Y., Konishi, H., Blair, B. G., Abukhdeir, A. M., Gustin, J. P., Rosen, D. M., Denmeade, S. R., Rasheed, Z., Matsui, W., Garay, J. P., Mohseni, M., Higgins, M. J., Cidado, J., Jelovac, D., Croessmann, S., **Cochran, R. L.**, Karnan, S., Konishi, Y., Ota, A., Hosokawa, Y., Argani, P., Lauring, J. & Park, B.H. (2013). "Single Copies of Mutant *KRAS* and Mutant *PIK3CA* Cooperate in Immortalized Human Epithelial Cells to Induce Tumor Formation." *Cancer Research*, *73*(11): 3248-61.

Cochran, R., Lauring, J., & Park, B. H. (2013). "TORn in Two Over Breast Cancer Drug Resistance." *ONCOLOGY*, *27*(1): 3–5.

Konishi, H., Mohseni, M., Tamaki, A., Garay, J. P., Croessmann, S., Karnan, S., Ota, A., Wong, H. Y., Konishi, Y., Karakas, B., Tahir, K., Abukhdeir, A. M., Gustin, J. P., Cidado, J., Wang, G. M., Cosgrove, D., **Cochran, R.**, Jelovac, D., Higgins, M. J., Arena, S., Hawkins, L., Lauring, J., Gross, A.L., Heaphy, C.M., Hosokawa, Y., Gabrielson, E., Meeker, A.K., Visvanathan, K., Argani, P., Bachman, K.E. & Park, B.H. (2011). "Mutation of a single allele of the cancer susceptibility gene *BRCA1* leads to genomic instability in human breast epithelial cells." *Proceedings of the National Academy of Sciences of the United States of America*, 108(43): 17773–8.

Cochran, R., Kalisiak, J., Küçükkilinç, T., Radic, Z., Garcia, E., Zhang, L., Ho, K.-Y., Amitai, G., Kovarik, Z., Fokin, V. V, Sharpless, K. B., & Taylor, P. (2011). "Oxime-assisted acetylcholinesterase catalytic scavengers of organophosphates that resist aging." *The Journal of Biological Chemistry*, *286*(34): 29718–24.

Küçükkilinç, T., **Cochran, R.**, Kalisiak, J., Garcia, E., Valle, A., Amitai, G., Radić, Z., & Taylor, P. (2010). "Investigating the structural influence of surface mutations on acetylcholinesterase inhibition by organophosphorus compounds and oxime reactivation." *Chemico-Biological Interactions*, *187*(1-3): 238–40.

Zou, J., **Cochran, R.**, & Cheng, L. (2010). "Double knockouts in human embryonic stem cells." *Cell Research*, *20*(3): 250–2.

Invention Disclosure

High-throughput Immortalization Ligation-free Amplification & Nominal DNA Error Rate (HILANDER). Park, B.H., Cravero, K.C., Chu, D. and **Cochran, R.L.** (Disclosure filed March 2014)